

Rational Design of a Low-Solvating Non-Flammable Electrolyte for Na-ion/metal Batteries.

A Thesis

submitted to

Indian Institute of Science Education and Research Pune in partial fulfilment of the requirements for the BS-MS Dual Degree Programme

by

Kumar Ashutosh



Indian Institute of Science Education and Research Pune

Dr. Homi Bhabha Road,
Pashan, Pune 411008, INDIA.

April, 2024

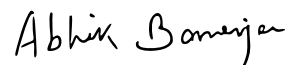
Supervisor: Dr. Abhik Banerjee

Kumar Ashutosh

All rights reserved

Certificate

This is to certify that this dissertation entitled **Rational Design of a Low-Solvating Non-Flammable Electrolyte for Na-ion/metal Batteries** towards the partial fulfilment of the BS-MS dual degree programme at the Indian Institute of Science Education and Research, Pune represents study/work carried out by Kumar Ashutosh at TCG-CREST Research Institute for Sustainable Energy, Kolkata under the supervision of Dr. Abhik Banerjee, Principal Scientist, Department of Chemistry, during the academic year, 2023-2024.



Dr. Abhik Banerjee

Committee:

Name of your Guide: Dr. Abhik Banerjee

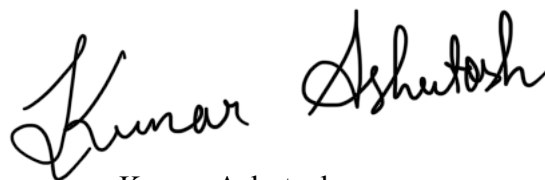
Name of Your TAC : Dr. Ramanathan Vaidhyanathan

This thesis is dedicated

To my father who told me to be a face in the crowd and my mother who shaped me to remember and follow it. My sister, to whom I am proud to be called her brother.

Declaration

I hereby declare that the matter embodied in the report entitled **Rational Design of a Low-Solvating Non-Flammable Electrolyte for Na-ion/metal Batteries** are the results of the work carried out by me at the Department of Chemistry, Indian Institute of Science Education and Research, Pune, under the supervision of Dr. Abhik Banerjee and the same has not been submitted elsewhere for any other degree.

A handwritten signature in black ink, reading "Kumar Ashutosh". The signature is written in a cursive, flowing style.

Kumar Ashutosh

Date: 15.03.2024

Table of Contents

1. <u>Abstract</u>	8
2. <u>Acknowledgments</u>	9
3. <u>Chapter 1 Introduction</u>	10
1.1 Batteries.....	11
1.2 Why Shift from Li-ion to Na-ion Batteries.....	13
1.3 Electrolytes for Na-ion Batteries.....	14
1.4 Salts for Na-ion Batteries.....	16
1.5 Solvents for Na-ion Batteries.....	19
1.6 How does solvents dissolve salts.....	20
4. <u>Chapter 2 Materials and Methods</u>	22
2.1 NMR Spectroscopy.....	22
2.2 Raman Spectroscopy.....	23
2.3 Synthesis of Battery-grade NaPF ₆ salt.....	24
2.4 Electrolyte Preparation.....	26
2.5 Coin-cell Fabrication.....	27
2.6 Cell-performance Analysis.....	29
GCD.....	
LSV.....	
2.7 Electrochemical Impedance Spectroscopy....	31
2.8 X-ray Photoelectron Spectroscopy.....	32
5. <u>Chapter 3 Results</u>	33
6. <u>Chapter 4 Discussion</u>	42
7. <u>References</u>	49

List of Tables

Table 1. Common Sodium salts structure and their physical property.....10

Table 2. List of commonly used solvents for LIBs and SIBs.....10

Table 3. Solubility chart of NaBF₄ and NaPF₆ salt in various Low-solvating solvents.....10

Table 4. Describes the circuit elements and their responses to frequency.....10

List of Figures

Figure 1. A Schematic Depiction of a SIB with HC anode and Layered Oxide Cathode. Anions and electrons are omitted for simplicity.

Figure 2 Physico-chemical, Economic Properties Comparison chart of Li⁺ vs Na⁺.

Figure 3. Multi-angle Radar plot comparison of various types of electrolytes.

Figure 4. HOMO-LUMO correlation with Oxidation-Reduction stability of an electrolyte.

Figure 5. Graphical Illustration of Solvation shell and strategies to design them.

Figure 6. A NMR plot highlighting the regions of chemical shift with respect to TMS reference. *Source:- <https://shorturl.at/cfqN0>.*

Figure 7. Depiction of all types of Elastic and inelastic scattering.

Figure 8. CR2032 coin cell components. *source-Yee, Youngki. “Recyclability of lithium ion battery materials.” (2017).*

Figure 9. Image of the Neware GCD-TESTER

Figure 10. Schematic of LSV technique and its application in electrolyte stability testing.

Figure 11. Detailed Nyquist Plot Representation Of Different Circuit Elements Possible In An Electrochemical Cell.

Figure 12. ^{31}P NMR(162 MHz), 0.1mmol NaPF_6 in 0.6 mL CD_3CN our result with respect to literature data from [38].

Figure 13. ^{19}F NMR(376 MHz), 0.1mmol NaPF_6 in 0.6 mL CD_3CN our result with respect to literature data from [38].

Figure 14. ^1H NMR(400 MHz), 0.1mmol NaPF_6 in 0.6 mL CD_3CN our result with respect to literature data from [38].

Figure 15. (a) Solubility difference between 1M NaPF_6 in DG of as Synthesized NaPF_6 (left vial) vs Commercially available NaPF_6 salt (right vial). (b) Measured Yield of NaPF_6 salt.

Figure 16. LSV plots for 1M NF (Red line) and 1.1M NFDF (Blue line).

Figure 17. Rate Performance plot for (a) 1M NF and (b) 1.1M NFDF.

Figure 18. A plot of Charge/Discharge Capacity Density for (a) 1 M NF and (b) 1.1 M NFDF.

Figure 19. Nyquist plots of impedance analysis after every C-rate of (a) 1M NF and (b) 1.1M NFDF.

Figure 20. GCD plot of (a)1 M NF and (b) 1.1M NFDF at 0.1 C for long cycling stability.

Figure 21. Raman spectra of (a) DME ether region along with the 1.1 M NFDF and (b) FTEP align with 1 M NF and 1.1 M NFDF.

Figure 22. ^1H Coaxial NMR (400 MHz), 1 M NaPF_6 in DG with D_2O as reference.

Figure 23. Non-flammability tests of (a) 1 M NaPF_6 in EC:DEC (1:1) and (b) 1.1M NFDF.

Abstract

Exponential reduction in Lithium reserves is an alarming indicator for requirement of alternate energy storage solutions to reduce the dependency on Lithium-ion Batteries. Sodium-ion batteries are considered as the most-promising replacement to Lithium-ion batteries. Electrolytes are the major components of the battery that contribute to its safety. Electrolyte is the major component of the battery that contributes to its safety. Most commercial LIBs have safety issues due to flammable electrolyte. SIBs in order to be better than LIBs need to be non-flammable in nature. The resulting two decades of research on electrolytes for SIBs have focused on this aspect, while not compromising on the performance. Therefore, research on electrolytes has relied on the SEI theory to optimize the components of electrolytes.

This thesis focuses on developing a low-solvating and a non-flammable electrolyte with exceptional cycling stability. The NVP||Na cells of the designed non-flammable electrolytes had a capacity fading of only 3% after 75 cycles as of now in comparison to 70% capacity fading of the base electrolyte within the above-mentioned number of cycles. This project also involved the synthesis of Battery-grade Sodium Hexafluorophosphate (NaPF_6 salt) due to its poor-quality commercial supply. The yield was calculated to be more than 96%.

Acknowledgement

“Time flies like an arrow, once released can never be called back.”

First of all, I would like to thank Dr. Satishchandra Ogale for giving me this opportunity and providing exceptional facility at TCG-CREST RISE. I would like to thank Dr. Abhik Banerjee for mentoring and improving me in academia at all prospects. Dr. Ogale and Dr. Banerjee play a very vital part in shaping me at present, which will greatly help me in future endeavors.

Secondly, I would like to thank all my lab-mates at TCG-CREST RISE for always helping me in sharing the lab-equipment whenever I needed them. Special thanks to Sreerop, Darshan, Shrestha, Himanshi and Srija for helping me with the background knowledge essential for this project and I am glad to be with these excellent people as I spent most of my lab space and time with them.

I would like to acknowledge and specially thank Mr. Newton Roy for his self-less help and mentoring me round the clock throughout my thesis project. This thesis would not have been complete if not received help from him.

Lastly, I would like to thank *Maa* who nurtured me, educated me and guided me throughout my life. Thank you *Papa*, who provided me with everything to climb up the stage and perform. Thank you Didi, for being the best sibling in the world and giving me key life lessons.

Thank you to my friends and family for being a part of this journey.

Enjoy reading my thesis work !!

Kumar Ashutosh.

Chapter 1 Introduction

The progressive depletion in non-renewable resources i.e. Fossil fuels, brings about the Energy Crisis in today's world. Since renewable energy cannot meet the demands in the current scenario. We need effective energy storage solutions to store these energies which can be used according to our convenience. Over the due course, various types of Energy storage devices such as Capacitors, Supercapacitors, Thermal Energy Storage, Batteries, etc. have been extensively researched to address this issue. Batteries of all have emerged to perform better than others in respect to its vast applications owing to their superior Energy density, Long Cycle Life, slow Discharge rate, Cost, etc ¹. With the growing energy demand and limited supply of lithium reserves ^{2,3}, there is a need for alternate, environmentally friendly and cost-effective sources of energy storage in order to reduce the sole dependence on LIBs ⁴. Sodium-ion batteries (SIB) are a type of rechargeable battery that use sodium ions instead of lithium ions as the charge carrier. Sodium is more abundant and less expensive than lithium, making SIB a promising alternative for large-scale energy storage systems. Also, SIBs have a lower environmental impact because they do not rely on critical or environmentally damaging materials like cobalt, which is commonly used in LIBs ^{5,6}. Despite a similar atomic structure, Sodium is much heavier than Lithium and has a lower Standard Electrochemical Potential compared to Lithium. These factors result in lower energy density compared to LIB.

Electromobility has been a growing interest in today's world ⁷. This requires batteries to be portable and most importantly safe. Electrolytes majorly contribute to the safety of a battery. There are mainly 3 types of electrolytes namely:- Solid-state Electrolytes, Polymer Electrolytes and Liquid Electrolytes. The former of these listed 3 electrolytes, i.e. Solid-state electrolytes, have serious challenges such as poor Ionic Conductivity, High interfacial resistance. Whereas polymer electrolytes have fabrication challenges and poor Ionic Conductivity. Therefore, Liquid electrolytes can be tailored for suitable applications due to their advantageous physio-chemical properties. However, Organic liquids come

with various challenges, one of which is its high-flammability and SEI dissolution properties.

Herein this Thesis I have focused on studying the properties of different electrolyte systems in order to synthesize, design and test a Non-flammable Electrolyte which can be used in Sodium-ion/metal/batteries. The resulting summation picture allows a critical evaluation of advantages and drawbacks of electrolytes for SIBs.

1.1 Batteries

Batteries are a closed thermodynamic system which can convert chemical energy into electrical energy and can be re-charged by changing the direction of electrons. The first battery known to humans was made at the end of the 18th century by Alessandro Volta at the university of Pavia, Italy. This battery consisted of a stack of alternating sequences of zinc and silver disks separated by clothes soaked in brine solution⁸. Since then, many different chemistries and forms of batteries have been developed. Batteries are broadly divided into two categories: Primary and secondary. Primary batteries are the ones that can deliver electricity from chemical reactions inside them only once. Whereas secondary batteries, or more commonly known as rechargeable batteries can supply electrical energy for more than hundreds of charge-discharge cycles. This thesis work will only consist of rechargeable batteries. Fig 1 is a schematic depiction of a SIB with Hard Carbon (HC) as anode and a Layered Oxide as Cathode.

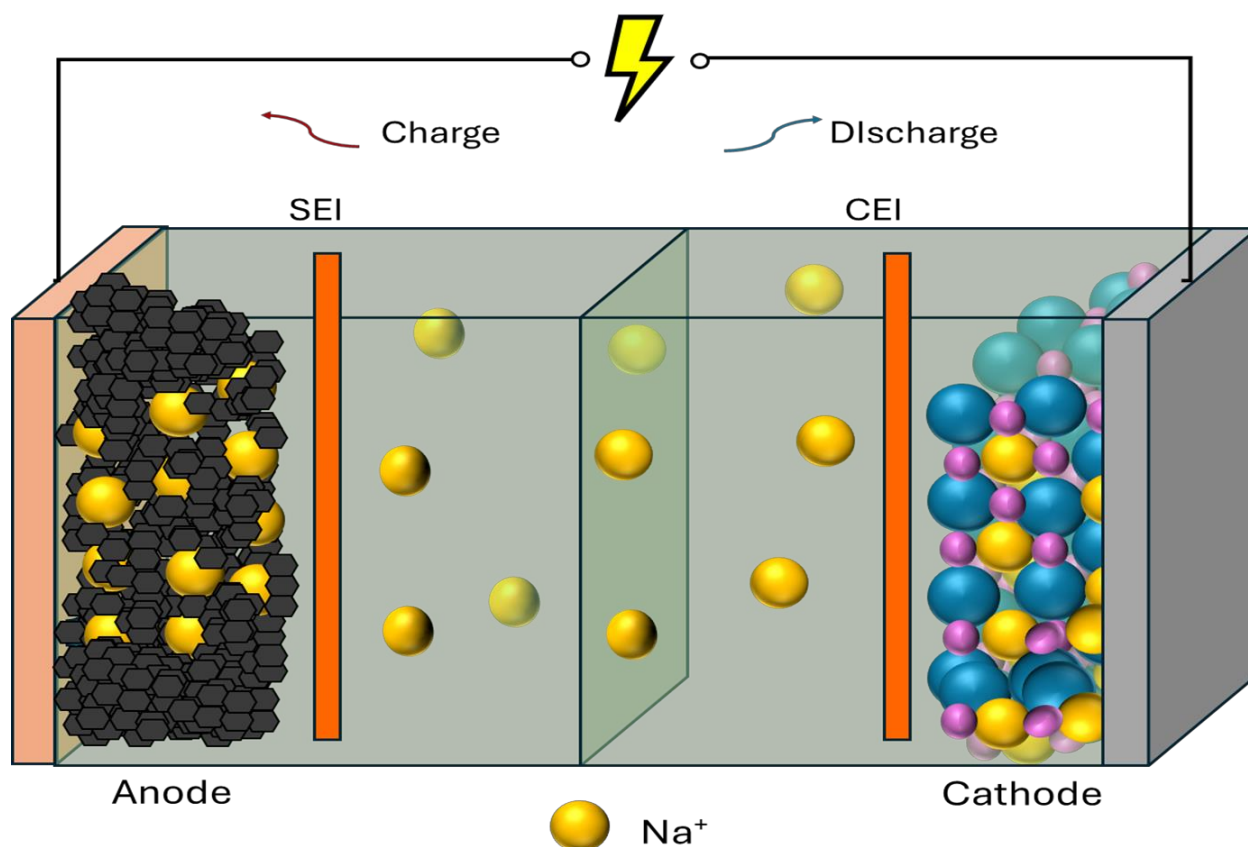


Fig 1. A Schematic Depiction of a SIB with HC anode and Layered Oxide Cathode. Anions and electrons are omitted for simplicity.

To be more specific, Battery is a device which is a pack of one or more electrochemical cells but in this thesis, they will be addressed interchangeably.

The main chemical phenomena governing the battery chemistry is redox reaction (reduction and oxidation) *at the interface* of two electrodes⁹. In a SIB, Sodium ion shuttles between the two electrodes during charge and discharge processes. During the discharge process, Oxidation of redox-active species occurs, and the electrons are liberated to the external circuit to flow towards the positive electrode or cathode doing work. To balance the flow of electrons, sodium/cations flow from anode to cathode where the reduction takes place. During the charging process, the above-mentioned mechanism is reversed. The electrodes are separated by a porous separator to prevent them from contact and resulting in short circuit¹⁰. In order to allow the movement of cations electrolyte is poured in between the electrodes for facile transport of these ions and not electrons.

1.2 Why Shift from Li-ion to Na-ion Batteries

LIBs were first commercialized by SONY in 1991. On account of more than 40 years of extensive R&D on LIBs, and the finding of new Lithium reserves have made them available for the masses at the cheaper cost. However, it is foreseen that Lithium availability may not fulfill the growing demand for energy storage devices in near future. Thus, the need for an alternative, cheap, and more sustainable energy storage device is essential. To this date, SIBs have a better and faster progress compared to other Beyond Li-ion Batteries, i.e. K/Ca/Mg-ion batteries.

This progress is attributed to two main causes: a) similar analogous chemistry to LIBs and b) same engineering and production equipment of LIBs ¹¹. The prototypes of SIBs have already been Demonstrated by TIAMAT (France), Faradion(UK), and CATL(China).^{12,13}

A high Specific Energy ~145 Wh/kg of SIBs using Hard Carbon anode and Inorganic materials as Cathode which is close to the commercial LiFePO₄||Graphite LIBs. This drives the further growing interest for the research on SIBs irrespective of lower Energy Density due to Higher mass and slightly higher reduction potential of Na⁺ compared to Li⁺ (-2.71 V vs -3.05 V vs SHE). Also, Li reacts with Al at lower potentials for which Cu current collector is used. But, this isn't the case with SIBs, So, Al current collector can be used on both electrodes making it more light-weight and cheap. ¹⁴

SIBs in order to meet the market demands and standards should be : a) thermally stable and safe, b)Fast charging suitable, c)very minimal Self-discharge when left at rest ¹⁵. To achieve these standards, an extensive and thorough R&D should be carried out on liquid electrolyte which are the main causes for safety concerns because of leakage, flammability reasons.

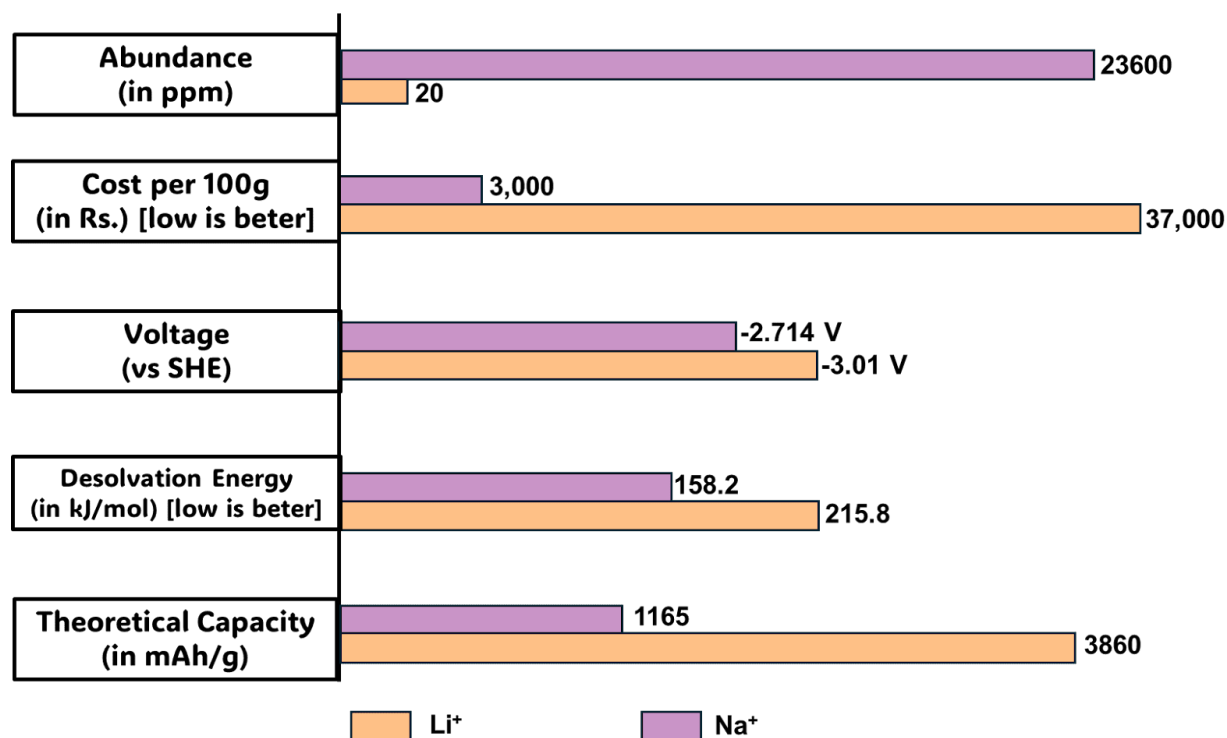


Fig 2. Physico-chemical, Economic Properties Comparison chart of Li⁺ vs Na⁺

1.3 Electrolytes for Na-ion Batteries

Electrolytes are a major component of a SIB since it allows diffusion of Na⁺ ions from cathode to anode through it and vice-versa while prohibiting the flow of electrons through them¹⁶. Till this end, three types of electrolytes have been investigated, namely Solid-state electrolyte ¹⁷, Polymer electrolyte ¹⁸ and Liquid electrolyte ⁵. The former of these have Interfacial resistance, poor compatibility with electrodes and also prone to cracking and causing defects whereas polymer electrolytes have poor ionic conductivity, narrow electrochemical stability and fabrication issues associated with it. To counter these issues research has been carried out on liquid electrolytes because of their flexible molecular-level engineering freedom.

Currently many liquid electrolytes are under R&D such as Ionic Liquids, Aqueous Electrolytes and Organic electrolytes, etc. Organic electrolytes have emerged as a comprehensive winner of them because of its unique properties such as high ionic conductivity, wide ESW and good compatibility with the electrodes.

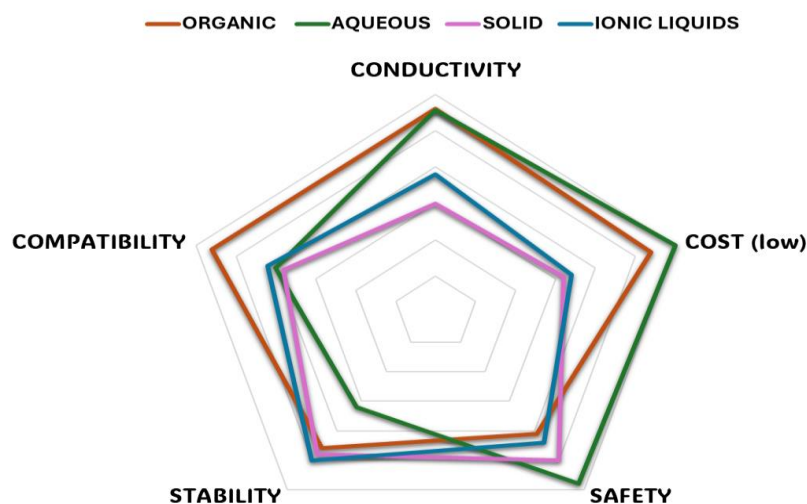


Fig 3. Multi-angle Radar plot comparison of various types of electrolytes.

Focusing only on the Non-aqueous Organic liquids, Ether-based and carbonate based electrolytes are two main-categories. Carbonate-based electrolytes were primarily preferred as ideal candidates as evident from commercial LIBs electrolyte (1 M LiPF₆ in EC:DEC). However, their further application to SIBs is hindered because of continuous dissolvable and thickening of SEI rooting from continuous degradation of carbonates.

In order to be incorporated as an ideal electrolyte, liquid electrolyte should match some end-user criteria: - a) High Ionic Conductivity, b) Large ESW, c) Thin, Robust, dense SEI, d) Non-flammable and thermally stable. This will be discussed in more detail in the next section. ¹⁹.

1.3.1 Liquid Electrolytes for SIBs

Liquid electrolytes as previously mentioned serves as the ion transport medium between the cathode and the anode. It comprises a source of Na⁺ (usually salts) and a medium (solvent) where Na-ion can migrate from one end to another.

In order to be an ideal electrolyte, It should have: -

- I. **High Ionic Conductivity (σ)** - High Ionic conductivity at least $\sim 10^{-3} \text{ S cm}^{-1}$ at Room-temperature (R.T) for facile movement of Na-ions. This factor is affected by multiple factors such as Viscosity, Salt concentration, etc. General thumb rule is that short linear molecules with good dipole-moment have relatively high conductivity. Also, increasing branching in an organic molecule/solvent increases Viscosity, hence, affecting conductivity of the electrolyte. ²⁰
- II. **Large ESW** - The ESW is a measure of the extent of an electrolyte to be stable to an oxidation or reduction reaction at a particular potential. It is a crucial factor to determine the stability of an electrolyte with respect to applied potential. ESW evaluation also helps in determination of a suitable set of electrodes which also reflects on energy density offered by the battery. Usually, a general thumb rule is a wider ESW, reflecting a higher energy density by use of more voltage difference electrode materials. ESW are generally related to the electronic states of the solvents and solvated cations against the applied voltage, i.e the relative Highest Occupied Molecular Orbital(HOMO), and the Lowest Unoccupied Molecular Orbital (LUMO) levels ²¹.

According to the *Goodenough* model, the ESW of an electrolyte can be determined by the difference of their HOMO and LUMO. A HOMO being electron-rich shows electron-donor ability due to the loose binding of electrons with nucleus whereas LUMO being electron-deficient exhibits an electron-acceptor property.²²

A higher LUMO infers that it is difficult to accept or gain electrons which signifies its superior reduction stability. Similarly a lower HOMO signifies it is difficult to extract electrons from the level leading to more oxidation stability. Since Anode is at a higher level and Cathode is lower in energy level diagram, LUMO would attribute to Reduction potential at the anode and HOMO to Oxidation potential. A higher LUMO will also refer to be reduction stable at the Anode, whereas lower HOMO will signify oxidation stability of species in the Cathode.

However, recent studies have found that the ESW as a difference of HOMO-LUMO (According to Goodenough *et al*) is an over-estimation of ESW. This is evident

from the fact that decomposition of the electrolyte to form a protective film on the electrodes is the reason for the success of rechargeable batteries²³. Fig 3. Summarizes the HOMO-LUMO concept for ESW.

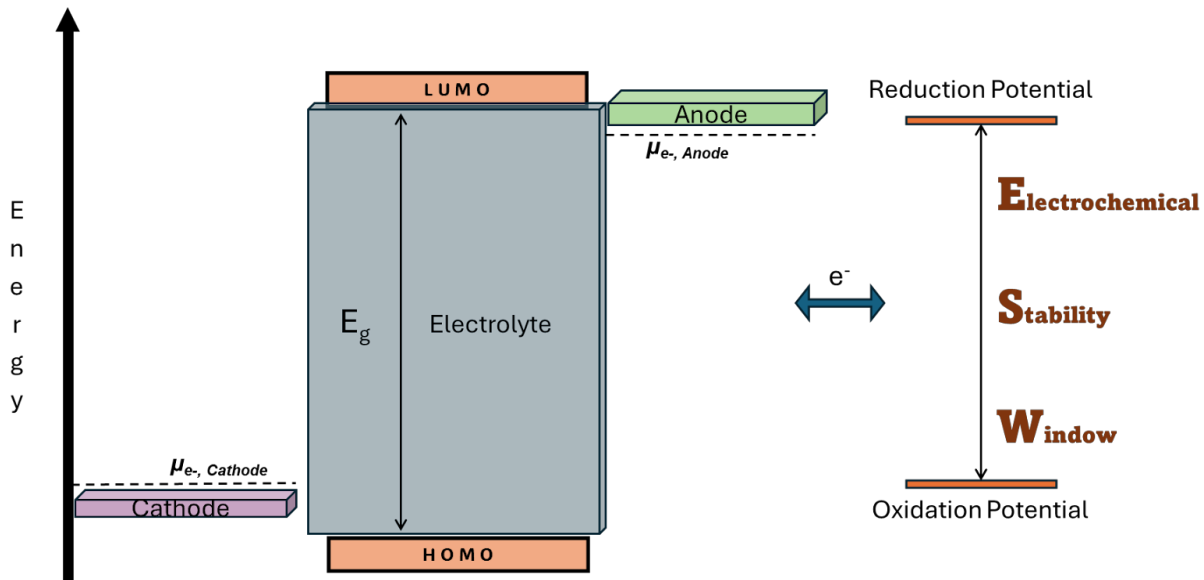


Fig 4. HOMO-LUMO correlation with Oxidation-Reduction stability of an electrolyte.

- III. **Robust SEI** - It is expected that the electrolyte as a whole should not decompose in the operation Voltage. But the success of the commercial batteries lies in the decomposition of electrolyte to form a protective film on the surface of the electrolyte. The protective film which is formed at the surface of the anode is called the Solid-Electrolyte Interphase (SEI) and the protective film at the surface of positive electrode is called the Cathode-Electrolyte Interphase (CEI).²⁴

The term SEI was first proposed by **Paled** in the year 1979²⁵ describing it as a electronically insulating and ionically conducting passivation layer on the interphase of electrode and liquid electrolyte. The SEI and CEI are formed during the initial charging cycles of the battery. These protective films should allow transport of ions but not electrons. Usually an inorganic-component-rich SEI is favorable for better cycle life, faster interfacial kinetics. In addition to this, the SEI layer should be thin, in order to lower resistance and be robust to prevent further decomposition (redox reactions) of electrolytes. Formation and evolution of the SEI

completely depends on the nature of the electrolyte composition; this will be further discussed in-detail ahead. The SEI/CEI should also have organic components in the composition since inorganic components (such as NaF, Na₂CO₃, etc) are fragile, Organic components give mechanical rigidity and support to the SEI/CEI layer.

- IV. **Non-flammable and in liquid state** - The electrolyte should be non-flammable to be used by the end-user and should be at liquid state for a wide range of temperatures. Usually phosphates are well adapted in the literature for being non-flammable additives/solvents. Detailed mechanism behind the non-flammability mechanism of phosphates will be discussed in the result and discussion section of this thesis. ²⁶

1.4 Salts for Na-ion batteries

Salts are inorganic crystalline compounds that consist of Na⁺ cations and anions packed in a crystalline lattice. Salts are the main source of Na-ions and require a solvent to dissolve them in order to liberate these ions. The salts should be chemically inert to the electrodes, thermally stable and most-importantly be cheap and Non-toxic.

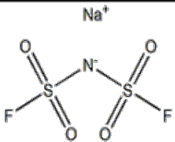
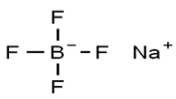
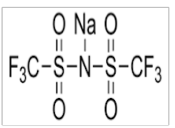
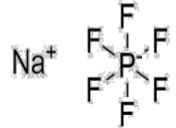
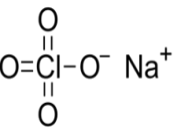
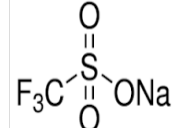
Name	Chemicals abbreviation	Structure	Melting Point (°C)	Name	Chemicals abbreviation	Structure	Melting Point (°C)
Sodium bis(fluorosulfonyl)imide	NaFSI		112	Sodium tetrafluoroborate	NaBF ₄		384
Sodium bis(trifluoromethanesulfonyl)imide	NaTFSI		204	Sodium hexafluorophosphate	NaPF ₆		200
Sodium Perchlorate	NaClO ₄		468	Sodium trifluoromethanesulfonate (Sodium triflate)	NaOTf		254

Table 1. Common Sodium salts structure and their physical property

1.5. Solvents for Liquid Electrolytes

Solvents are the medium which dissolves the salts and provides transport of Na⁺-ion through it between two electrodes. Some of the common organic solvents being used in Battery electrolytes are listed below.

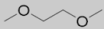
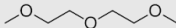
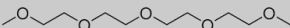
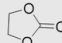
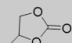
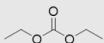
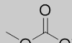
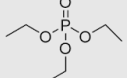
Solvent	Molecule structure	T _m (°C)	T _b (°C)	T _f (°C)	η	ε
DME		-58	84	7	0.46	7.2
DEGME		-60	162	57	1.06	7.4
TEGDME		-30	275	140	3.36	7.5
EC		36	248	160	1.9	89.7
PC		-48	242	132	2.53	64.9
DEC		-74	126	31	0.76	2.8
DMC		5	91	18	0.59	3.1
TEP		-56.4	215	115	1.56	13.01

Table 2. List of commonly used solvents for LIBs and SIBs

In general, Solvents can be divided into two main categories, High-solvating and low-solvating solvent. High-solvating solvents can dissolve more than 2 M of salts in them. This is because they are highly polar and donate electrons to dissolve the salt such as Carbonates. While low-solvating solvents cannot dissolve ≤ 2 M of salts. In ethers, it has been shown that decreasing O-atoms and increasing alkyl chains can decrease the solvating power of Ether solvents. This means that DME is more solvating than DEE (number of Oxygen) and DPE is low-solvating solvent than DEE (alkyl chain) ²⁷. For the SEI to be Anion-rich, low-solvating solvents are a must.

1.6. How do solvents dissolve Salts ? - The Solvation concept

Solvation is the interaction between the solvent with the dissolved solute (salt). This phenomena arises due to the competition between solvent molecules and the anions from the solute to bond with the cations. Solvent polarity is a major factor in determining to what extent it can dissolve a particular salt. Solvents which are polar in nature have molecular dipoles which means that they have particular portions in the molecule structure where the electron density is higher. Therefore, a partial negative charge is developed and a partial positive charge is developed on the portions with less electron density portions of the molecule. The polar solvent molecule can dissolve polar salts by orienting their partially negative charged portions towards the cations of the salt by means of electrostatic attraction. This process stabilizes the system and gives rise to a solvation shell which is basically wrapping up of ions (Na^+ ions here) by the solvent molecules. Solvation is a bond formation process, typically Hydrogen-bonds and van der Waals force.²⁸

It has been shown in literature that the solvation structure of the Na^+ -ion in the electrolyte dictates the formation and properties of the SEI and CEI layer.^{29,30} Conventional electrolytes concentration ($\leq 1 \text{ M}$) have a large amount of free solvent molecules compared to Anions. The solvation shell arising is a Solvent-separated Ion Pair (SSIP). On increasing salt concentration, Anion concentration also increases significantly. Since the competing free solvents molecules are less in comparison to anion number, the solvation shell arising in this scenario will be Contact-Ion Pair (CIP). In CIPs, Anions are coordinated to the cations inside the solvation shell. On further increasing the concentration ($> 2 \text{ M}$), Cation-anions bond cannot be separated by solvents resulting in Aggregate-Ion Pairs referring to presence of Cation-Anions aggregate inside one solvation shell.³¹

Studies show that electrolytes with SSIP species tend to form an Organic-rich SEI due to preferential reduction of Solvent molecules in the solvation shell. But, CIPs and AGGs containing electrolytes tend to form Inorganic-rich SEI for better ion-conductivity through the SEI. Also, a small amount of Organic components in SEI helps in providing mechanical stability to SEI.

Therefore, in order to achieve a Inorganic-rich SEI, Anion-derived SEI layer needs to be formed for which CIPs and AGGs species are necessary to be present in the electrolyte.

Fig below provides a visual illustration of the Solvation shell and the strategy to achieve them. ³²

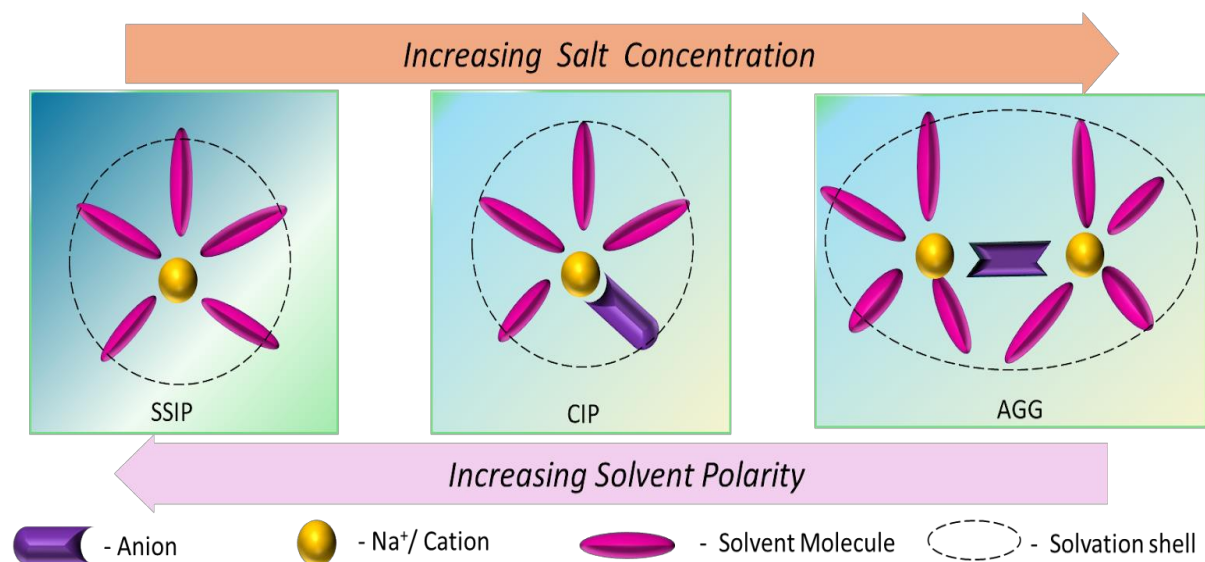


Fig 5. Graphical Illustration of Solvation shell and strategies to design them

Chapter 2 Materials and Methods

2.1. Nuclear Magnetic Resonance (NMR) Spectroscopy

NMR spectroscopy is a powerful analytical technique to study the dynamics and determine structure of molecules. It is used for identification of atoms based on the principle that atomic nuclei are charged species and have spins associated with them. All nuclei with an odd mass number like ^1H , ^{13}C , ^{19}F , ^{31}P have a spin angular momentum making them NMR active. The working of NMR basically involves placing the sample in an external magnetic field and then exciting it with pulsed radio frequency. The excited nuclei traverse a Free induction decay pattern unique to every nuclei according to their chemical surroundings. This pattern gives a distinct NMR signal corresponding to the sample.

A NMR signal is basically plotted as a chemical shift with respect to a reference point (TMS here). Area under the peak of a NMR signal signifies the number of species in the same chemical environment contributing to the chemical shift. Chemical shift can be calculated from the formulae given below, ³³

$$\delta = \frac{\text{frequency of signal} - \text{frequency of standard}}{\text{spectrometer frequency}} \times 10^6 \quad \dots\dots\dots(2.1)$$

Every nuclei has a definitive chemical environment. Electron density. The greater the electron density all around the nucleus, more is the opposition to the applied magnetic field by the electrons, and hence the greater the shielding. More shielded nuclei appear upfield or right to the x axis. Similarly, less shielded nuclei appear downfield or left side of the x-axis. More shielded nuclei require a stronger magnetic field to resonate and less shielded nuclei requires a weak magnetic field to resonate. This makes NMR a very-sensitive technique which helps in detecting the purity of the sample as well.

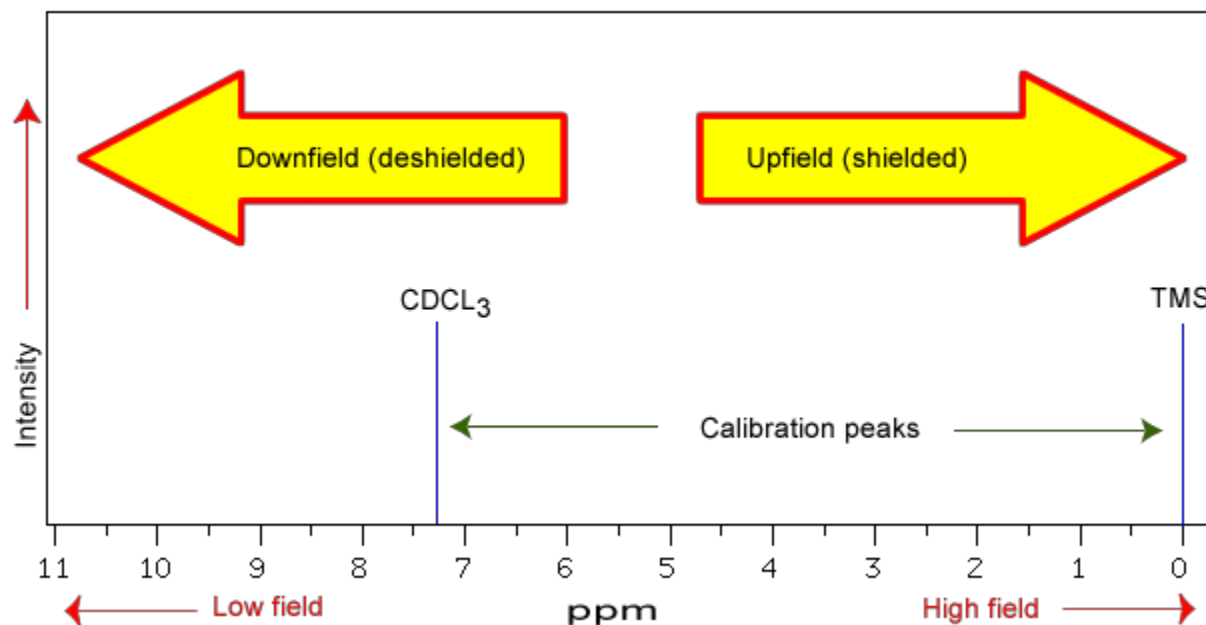


Fig 6. A NMR plot highlighting the regions of chemical shift with respect to TMS reference. *Source:-* <https://shorturl.at/cfqN0>

2.2. Raman Spectroscopy

Raman spectroscopy is a non-destructive analytical technique used to determine vibrational modes of a molecule. It is associated with the inelastic scattering of photons when a monochromatic light of a specific wavelength is shined upon the material. The photons of the monochromatic light source (*usually lasers*) upon interaction with molecules at different vibrational states distorts the electron cloud around the molecule resulting in inducing an electric Dipole moment P on the molecule.

$$P = \alpha \cdot E \dots\dots\dots(2.2)$$

This interaction results in the laser either gaining or losing energy. The laser interacts with the molecule transferring energy, leaving with a higher energy (*Anti-stokes*) which means energy is transferred from the molecule to the photon or leaving with a lower energy (*Stokes*) meaning transfer of energy from photon to molecule. These interactions gives a structural fingerprint which can be used to identify molecules. Fig 7. describes the above

explained interactions. Stokes scattering is usually preferred due to its higher probability and a better signal-to-noise ratio.

In liquid electrolytes, Raman spectroscopy is very useful to identify the presence of Ionic Solvation Species, i.e SSIPs, CIPs, etc. It is important to note that Raman effects are one-to-millionth (low) competing phenomena. So, a low energy laser such as **532 nm** laser) should be used to avoid other phenomena such as Fluorescence. The liquid samples are packed and sealed in a NMR tube and are examined during raman analysis.

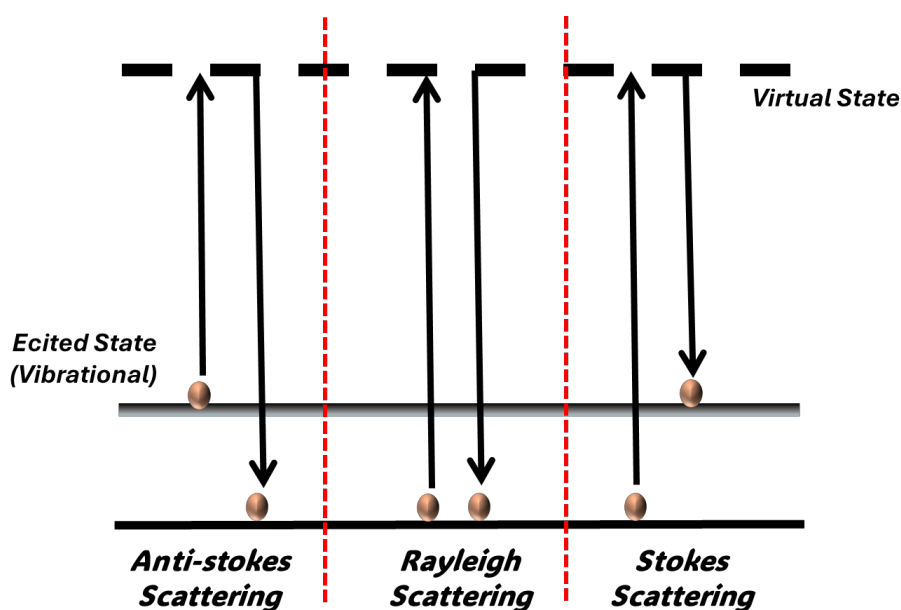


Fig 7. Depiction of all types of Elastic and inelastic scattering

2.3. Synthesis of Battery-Grade NaPF₆

NaPF₆ has some attractive properties which makes it a superior salt compared to other commonly used salts ³⁴. However, studies have shown that NaPF₆ is highly hygroscopic and undergoes hydrolysis readily to produce NaF, HF and insoluble phosphates species such as PO₄³⁻ ^{35,36}. This hydrolysis can take place even at moisture level < 20 ppm. This clearly serves as evidence for the poor quality of commercially available NaPF₆. The presence of impurities is a setback on battery research, as these insoluble hydrolysis products hinder the real electrolyte concentration and its true potential. Bhide and

Adelhelm reported that when using a high purity (99%) supply of NaPF₆, an insoluble fraction appeared beyond 0.4 M concentration when dissolving in EC:DMC 30:70 wt% ³⁷.

Herein, we have successfully synthesized pure battery-grade NaPF₆ using the precursors from the paper ³⁸, and developing our own easy-to-setup experimental setup.

- **Materials required** - Super-dry THF, Dry Hexane, NH₄PF₆ were purchased from Sigma-Aldrich (purity $\geq 99.98\%$), Sodium cubes were purchased from Sigma-Aldrich (purity $\geq 99.99\%$), Teflon-coated magnetic beads, Double-neck RB, reflux condenser, bladders, Long needles, Syringe filters, etc.

Synthesis of NaPF₆ was carried out by dissolving 10g of NH₄PF₆ (61 mmol, 2 *equiv.*) in 40 mL of THF inside Inert conditions in R.B. Sodium was put out of mineral oil and washed with hexane to remove the oil. Equimolar ratio of Na-metal was transferred into double-neck R.B with magnetic beads. The Na-pieces were further washed with Hexane and dried to remove any residual oil. 10 mL THF was poured into the RB containing Na-metal. Both R.Bs were packed inside an Ar-filled Glovebox with H₂O and O₂ <0.1 ppm. The R.Bs were brought outside the Glove Box for the reaction procedure.

NH₄PF₆ dissolved in THF was added dropwise using a long needle-syringe to Na-metal suspended in THF. The reaction is very vigorous and effervescence is observed. After all the addition has been done, the reaction mixture was allowed to stir at ambient temperature (R.T) for 1 hour. Following this, a reflux condenser was fitted and the reaction mixture was heated to reflux for 7 hours. After this, the temperature is decreased to 50° C and stirred for 16 hours. Following this the liquid part is extracted out using syringe-filters and transferred into a fresh R.B. The solvent is evaporated using *Rotary-Evaporation* to obtain white product. The powder is further dried under vacuum in Buchi-furnace in order to obtain NaPF₆ salt.

2.4. Electrolyte Preparation

Preparation of non-aqueous liquid electrolyte requires dry salts and solvents. It should be carried out inside a Ar-filled Glovebox with H₂O and O₂ content <0.1 ppm to prevent further contamination by moisture. The salt was weighed and transferred into a clean vial and solvent was poured sequentially to obtain the desired molarity. The solvents were dried using Molecular sieves(4 Å) overnight before preparing electrolyte. Similarly, the salts were pre-heated under vacuum for overnight before being used. The mixture was stirred on a magnetic stirrer for at least 6 hours before adding any additive. The electrolyte with all the components were stirred overnight before being used for preparing coin-cells.

This thesis includes a solubility chart showing the solubility of various salts in the low-solvating ethers,phosphates present in the lab.

Salt	Solvent name	Molarity	Solubility	Salt	Solvent name	Molarity	Solubility
Sodium Tetrafluoroborate (NaBF ₄)	Isoamyl Ether	1 M	NO	Sodium Hexafluorophosphate (NaPF ₆)	Isoamyl Ether	1 M	NO
		0.5M	NO			0.5M	NO
	tert-butyl Methyl Ether	1 M	NO		tert-butyl Methyl Ether	1 M	NO
		0.5 M	NO			0.5 M	NO
	tert-Butyl Ethyl Ether	1 M	NO		tert-Butyl Ethyl Ether	1 M	NO
		0.5M	NO			0.5M	NO
	sec-Butyl Ether	1 M	NO		sec-Butyl Ether	1 M	NO
		0.5 M	NO			0.5 M	NO
	Dipropyl Ether	1 M	NO		Dipropyl Ether	1 M	NO
		0.5M	NO			0.5M	NO
	Butyl-Ethyl Ether	1 M	NO		Butyl-Ethyl Ether	1 M	NO
		0.5 M	Sparingly Soluble			0.5 M	Sparingly Soluble
	Cyclohexyl Methyl Ether	1 M	NO		Cyclohexyl Methyl Ether	1 M	NO
		0.5M	NO			0.5M	YES
	Triethyl Phosphates	1 M	YES		Triethyl Phosphates	0.5 M	YES
	Dimethoxy Ethane	0.5 M	YES		Dimethoxy Ethane	1 M	YES
	Diglyme	0.5 M	YES		Diglyme	1 M	YES
	Tetraglyme	1 M	YES		Tetraglyme	1 M	YES
	F-Triethyl Phosphate	0.5 M	NO		F-Triethyl Phosphate	0.5 M	NO

Table 3. Solubility chart of NaBF₄ and NaPF₆ salt in various Low-solvating solvents.

Preparation of the non-flammable electrolyte - 1.5M of NaFSI salt dissolved in F-TEP was first prepared in a clean vial. Then, DME was added to dilute the solution to the solvent ratio obtained as 3:1. Then 5 vol% FEC was added to obtain the final electrolyte as 1.1M NaFSI in FTEP:DME (3:1) + 5 vol% FEC. The prepared electrolyte will be hereafter addressed as **1.1M NFDF**. The base solvent for reference will be 1 M NaFSI in FTEP (abbreviated as 1M NF).

NaFSI was purchased from Solvionic Pvt. Ltd.(purity >99.9%), FTEP from CombiBlock Pvt. Ltd (purity >98%), DME from Sigma-Aldrich (purity >99.9%) and FEC from Solvionic (purity >99%) was purchased and used for the experiment.

2.5. Coin cell Assembly.

To test the performance of the as made electrolyte coin cells are the primary check to test its performance. A typical coin cell consists of a positive and a negative casing, a spring to pack all the components inside, two spacers both sides to allow for current flow, Electrodes coated on a current collector and a separator to prevent short-circuit.

The CR2032 coin cell components were washed with IPA and dried overnight in vacuum. Whatman GF-F separators were cut (19 mm) and dried in 120° C overnight. The drying process is a crucial factor in building Na-metal based cells to ensure no moisture contribution.

$\text{Na}_3\text{V}_2(\text{PO}_4)_3$ (NVP)/C was coated on a Carbon-coated Al-foil using the wet slurry coating process. The slurry composition was 80:10:10 of Active material:SuperP carbon black:Polyvinylidene (PVDF) binder respectively dissolved in N-methyl Pyrrolidone (NMP). The coating was dried in a 60° C oven under vacuum overnight. The coating was cut into small electrodes discs of diameter 14mm. All the components were packed and transferred into the glovebox for cell fabrication.

The cell fabrication was carried out in an inert and dry Glove Box with O_2 and H_2O content <0.1ppm. Na-metal will be used as anode material from hereon throughout the thesis. The Na-metal (inside Mineral oil) was washed with Hexane to remove oil from the surface and the oxide layer was removed with a ceramic knife to expose the shiny surface of Na-

metal. Thin and even Na-metal sheets were rolled from the cube of roughly 200-300 μm and then cut into discs of 10mm diameter. The anode is taken less to prevent edge-defect and dendrite growth during charge-discharge cycle. The Na-metal was placed at the center of the negative spacer. The coin assembly from the negative casing side as illustrated in the Fig. given below. During fabrication, *alignment* of electrodes is a crucial factor as a minute amount of misalignment may lead to loss of Na-metal inventory due to plating-stripping³⁹. The cell after all components assembly was crimped at 0.8 Ton using an automatic coin-cell crimper from MTI Pvt. Ltd. inside the glovebox and taken outside for further testing.

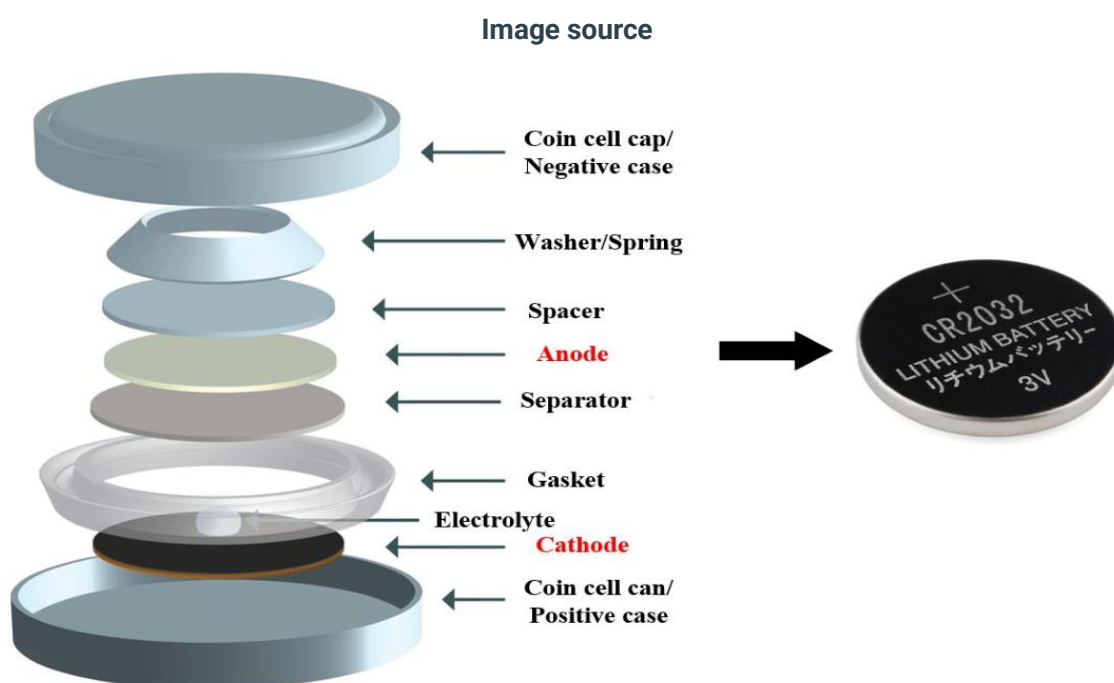


Fig 8. CR2032 coin cell components. *source-Yee, Youngki. "Recyclability of lithium ion battery materials." (2017).*

2.6. Cell-Testing Techniques

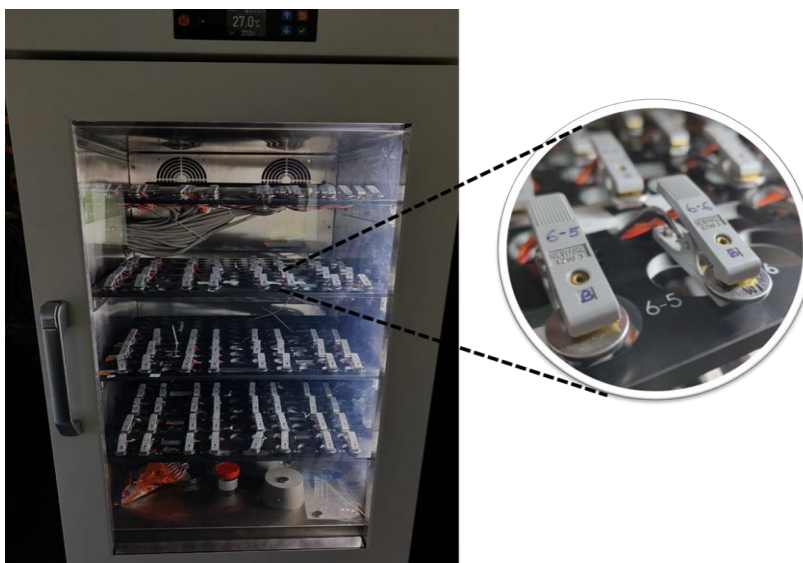
Galvanostatic Charge-Discharge Measurement

Charge-Discharge cycle is the primary test measurement carried out to check the stability and kinetics of an electrolyte. Charge-Discharge cycling was carried out using Neware Battery-Tester inside a constant temperature cabinet maintained at near R.T (300 K). The current-rate as per the name suggests is kept constant. This technique takes input of Voltage and current, and the voltage is swept from lower potential to higher potential and vice-versa during the charging and discharging processes respectively. Many fundamental measurements such as IR drop, C.E, Heat generated, Power, Capacity Density, etc. can be measured using this technique.

The current rate or C-rate can be defined as,

$$1C = \frac{\text{Active material loading/cm}^2 \times \text{Theoretical Capacity}}{1000} \dots\dots\dots(2.3)$$

where Theoretical capacity is the capacity of the limiting electrode, i.e. NVP which is 117 mAh g⁻¹. 1C is the current-rate at which the cell can be Charged and discharged at 1hr each. A 0.5C current rate means a battery is being charged and discharged at 2 hours each. Usually, Slow C-rate is applied initially for the formation of the SEI layer. Higher C-rate is applied in order to check the Kinetic limitations of the battery. Fig 9. Image of the Neware GCD-TESTER instrument.



Linear Sweep Voltametry

Linear Sweep Voltage or LSV is a technique used to measure the oxidation or reduction stability of a particular electrolyte vs Na^+/Na . In LSV, current is measured while the potential is swept linearly as a function of time. Voltage is swept as a function of time which is defined as the scan rate (V s^{-1}). LSV data is represented as anodic or cathodic current in the y-axes and Voltage vs Na^+/Na in the y axes. The LSV results are dependent on various factors such as :- 1) The scan rate, 2) Electrochemical reactivity of materials, 3) rate of electron transfer process. ⁴⁰

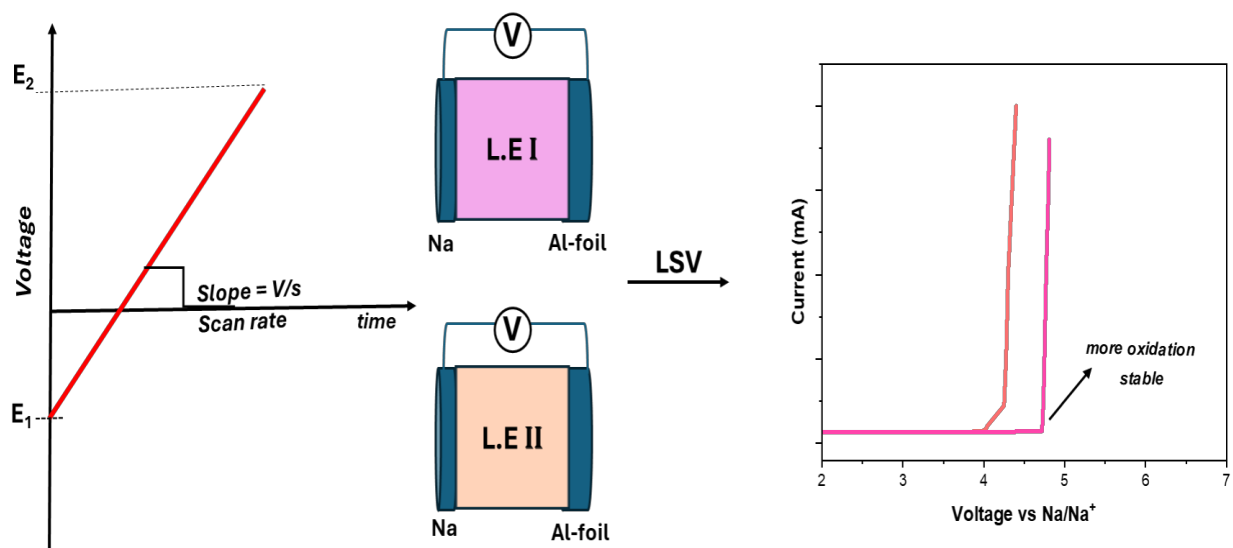


Fig 10. Schematic of LSV technique and its application in electrolyte stability testing.

2.7. EIS

Applying a constant Voltage across a resistor induces a constant current through the circuit. Similarly, a sinusoidal varying potential across an electrochemical cell will induce a sinusoidal current through it.

In impedance analysis, a sinusoidally varying potential (V_ω) is applied to an electrochemical state either in equilibrium or at steady state and the time-dependent current (I_ω) is recorded as a function of ω . The AC analogue of Ohm's Law is given by $V_\omega = I_\omega \times Z$ where Z is the impedance for V_ω and I_ω .

EIS simplifies a complex electrochemical cell by deconvoluting it into simple individual processes with different time-constants. A process occurring at a longer time scale can be probed to low frequency while fastest time-scale processes can be probed to high frequency.⁴¹

Element	DC	AC	Frequency Dependence	Z	θ
Resistor	+	+	Independent	R	0
Capacitor	Open circuit	+	Inverse relation	$1/\omega C$	-90°
Inductor	Short circuit	+	Direct relation	ωL	$+90^\circ$

Table 4. Describes the circuit elements and their responses to frequency.

EIS data are generally presented either as a Vector (Bode plot) or as a complex quantity (Nyquist plot). For the complex quantity,

$$Z_{\text{total}} = Z' \text{ (real)} + Z'' \text{ (Imaginary)} \dots \dots \dots (2.4)$$

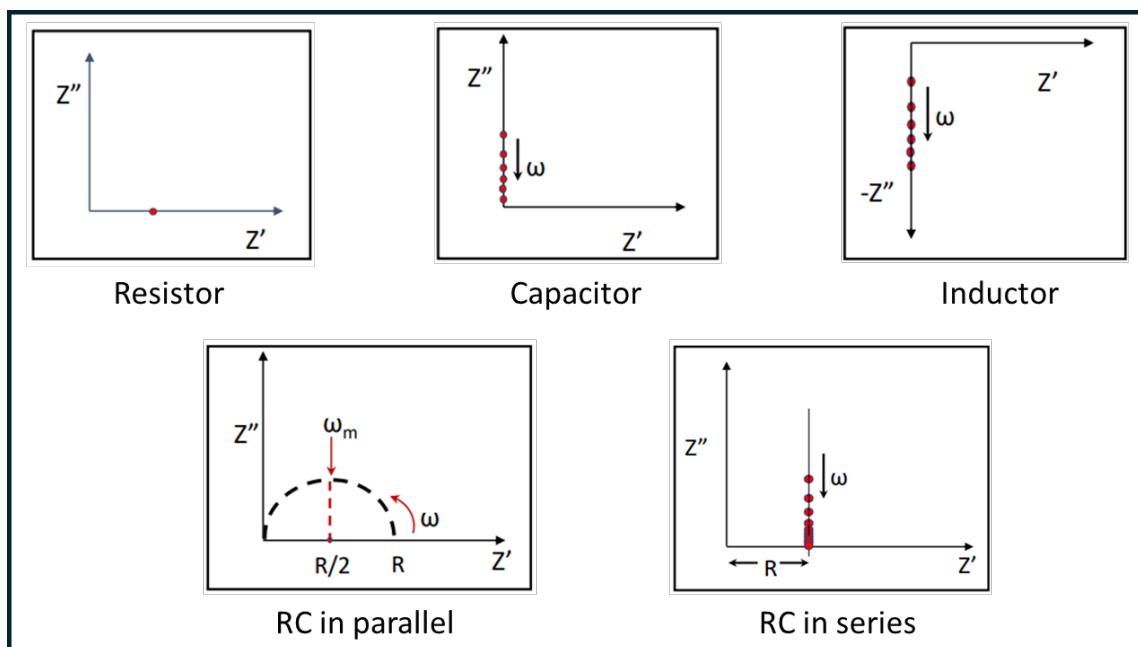


Fig 11. Detailed Nyquist Plot Representation Of Different Circuit Elements Possible In An Electrochemical Cell.

2.8 XPS (IF) -

X-ray Photoelectron Spectroscopy is a non-destructive spectroscopic technique used to study the surface of the solid material. It can be sensitive to a depth of 5-10 nm. It is a spectroscopy technique used to study the core shell electrons based on the photoelectric effect. XPS can detect all elements from Li to U except H and He since He is not present in solid state and the 1s orbital is very small for photoemission. XPS identifies elements based on the kinetics of the electrons emitted upon irradiation of a sample with X-ray. The bonding environment of an element greatly affects the binding energies of the corresponding elements ⁴². Faster moving emitted electrons, i.e. Higher kinetic energy signifies a lower Binding energies and vice versa. XPS can also be probed to study the oxidation states of elements. For example, in an NVP cathode, the electrochemical process is governed by the redox phenomena of V^{3+}/V^{4+} . The vanadium 4+ oxidation state can be detected using XPS soon after the charging process to observe an upward shift in the B.E (higher B.E value).

In this thesis XPS is being carried out for post-cycling characterization with respect to pristine cathode material to detect any structural change in Cathode.

Chapter 3 Results

Through this thesis I have screened, examined various electrolytes consisting of sodium-salts and Organic solvents and their role in determining the cell performance.

The first part of the project included Screening various concentrations of salts dissolved in Single organic solvents to find the highest molarity a particular Low-solvating solvent can dissolve as mentioned in Table.

The second part included synthesis of pure-battery grade NaPF_6 . After the Sodium-hexafluorophosphate was synthesized. The salt was dried under active-vacuum for 12 hours at 120°C using Buchi-furnace. The Buchi-furnace was sealed and transferred inside the Glove-box through the ante-chamber before being cooled. The vacuum was released inside Glovebox to ensure no transfer of air/moisture. The Salt was scratched out and NMR analysis was carried out to match the data with the Literature values. The solvent used was CD_3CN . ^1H NMR, ^{31}P , ^{19}F NMR were conducted at 295 K. The NMR plots are as follows.

- NMR data of ^{31}P

^{31}P NMR (162 MHz, CD_3CN , 295 K) spectrum of sodium hexafluorophosphate (0.1 mmol of NaPF_6 , 0.5 mL CD_3CN).

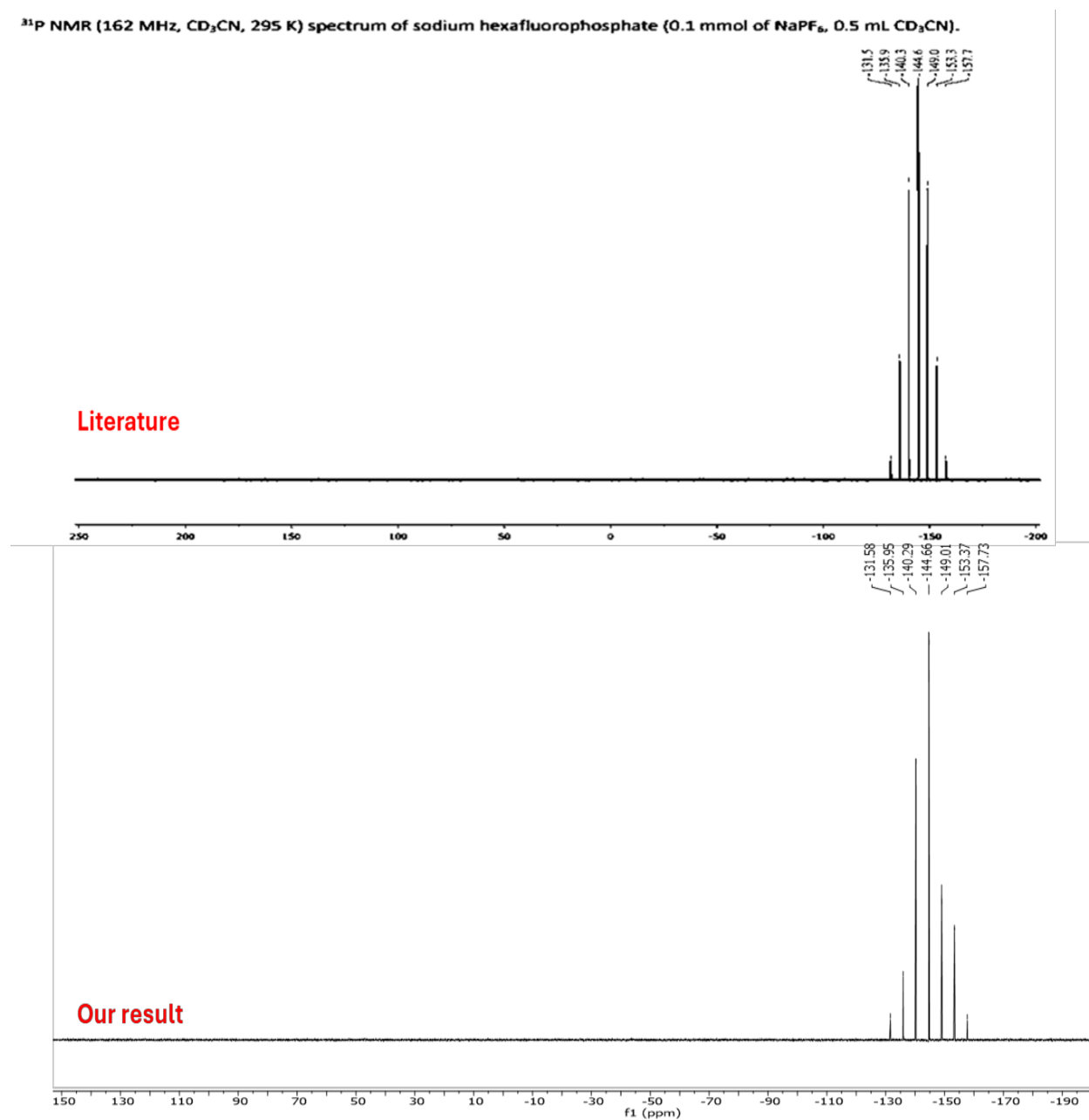


Fig 12. ^{31}P NMR(162 MHz), 0.1mmol NaPF_6 in 0.6 mL CD_3CN our result with respect to literature data from [38].

- NMR data of ^{19}F

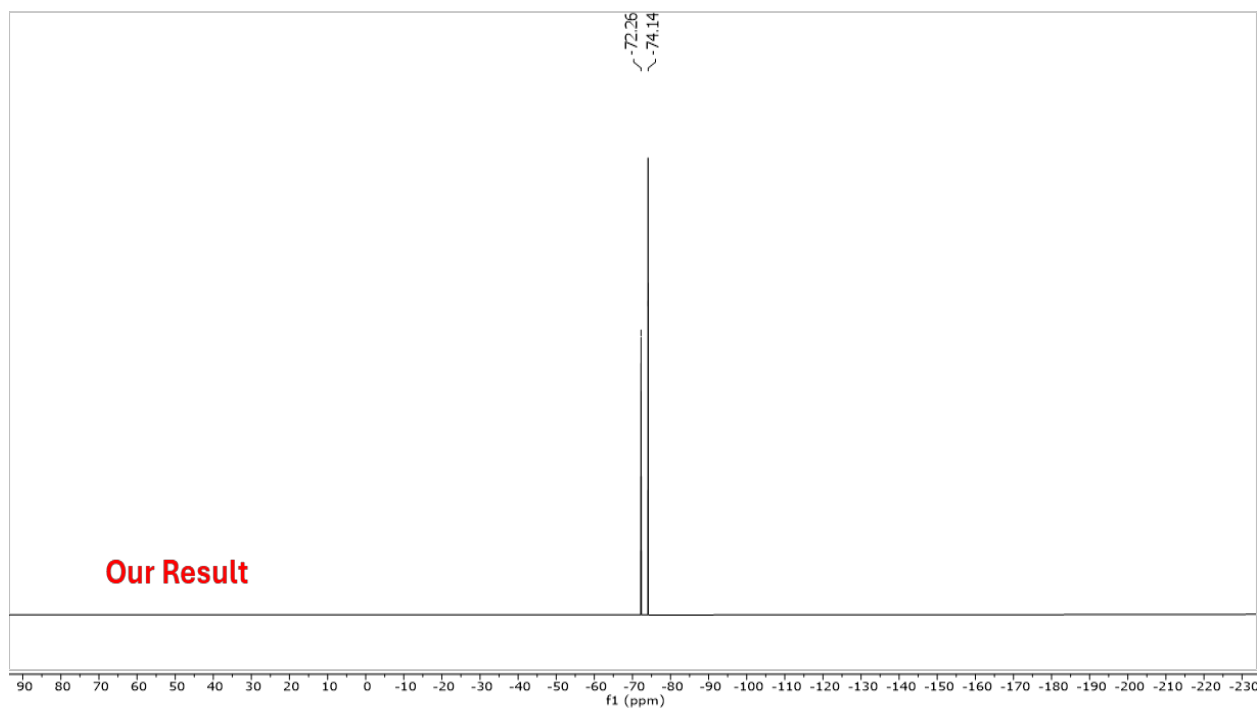
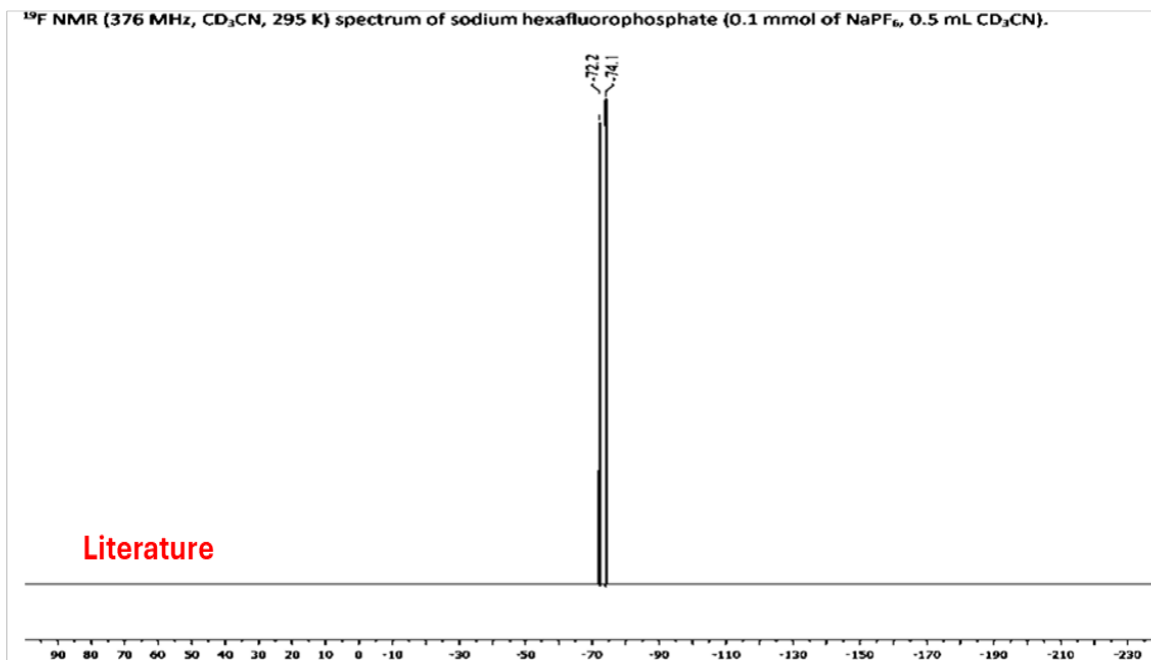


Fig 13. ^{19}F NMR(376 MHz), 0.1mmol NaPF_6 in 0.6 mL CD_3CN our result with respect to literature data from [38].

- NMR data of ^1H

Figure S2.1.3 ^1H NMR (400 MHz, CD_3CN , 295 K) spectrum of sodium hexafluorophosphate (0.1 mmol of NaPF_6 , 0.5 mL CD_3CN).

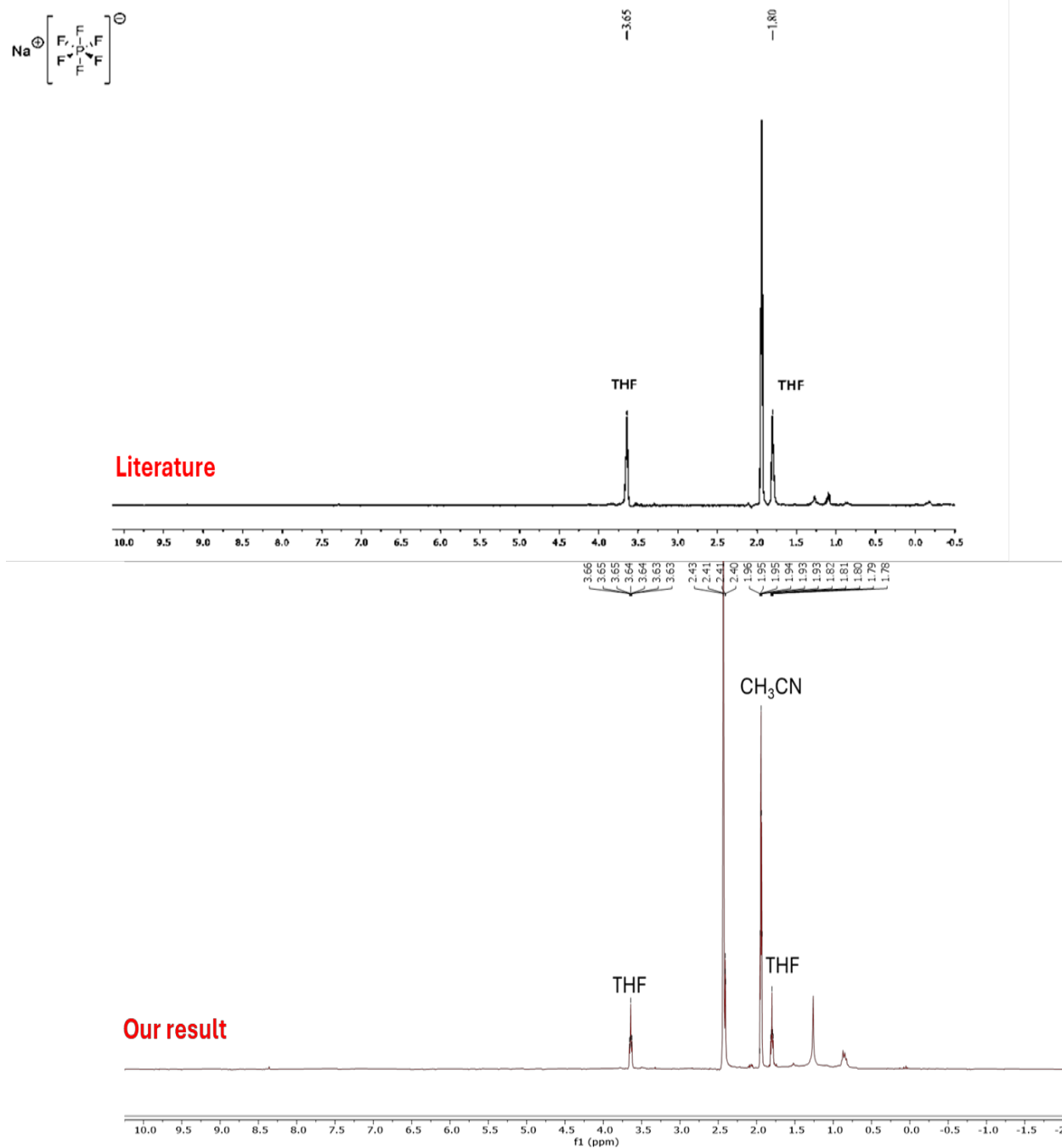


Fig 14. ^1H NMR(400 MHz), 0.1mmol NaPF_6 in 0.6 mL CD_3CN our result with respect to literature data from [38].

The extra peak is observed in ^1H spectra at 2.4 ppm which indicates further purification to be carried out. The further procedures are explained in the Discussion part.

The solubility of the new salt is drastically increased as evident from a comparison of 1M of Synthesized NaPF_6 in DG vs 1 M of Commercial NaPF_6 (purchased from Sigma-Aldrich) in DG. Yield was measured to be $\sim 9.6\text{g}$.

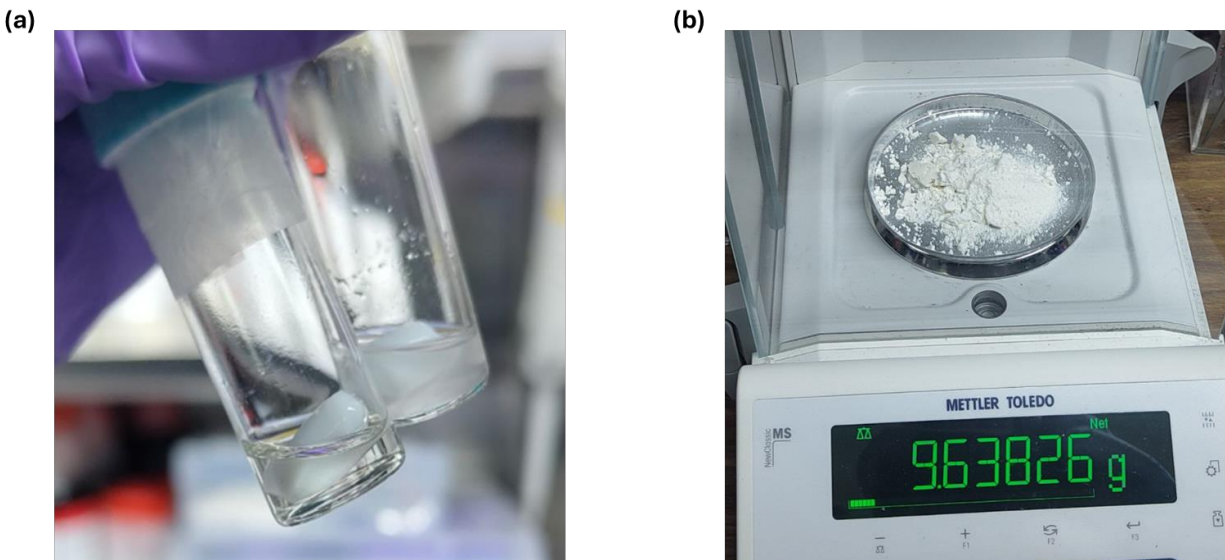


Fig 15. **(a)** Solubility difference between 1M NaPF_6 in DG of as Synthesized NaPF_6 (**left vial**) vs Commercially available NaPF_6 (**right vial**). **(b)** Measured Yield of NaPF_6 salt.

The third part of the project included selecting the Salt and bi-solvent mixture with Additives to make the Electrolyte which is non-flammable and Low-solvating in nature.

The electrolytes under study in this thesis are 1.1M NFDF and 1 M NF(Preparation procedure mentioned above). After overnight stirring, the electrolyte was undisturbed for 2 hours before the electrolyte was prepared. The electrolyte was clear and transparent. 150 μL of electrolyte was poured on the Separator for each cell and the cell was assembled as mentioned in protocol in the previous chapter. The cell was crimped at 0.8 ton to ensure the cell is properly sealed and no sign of leakage was observed.

For LSV, Na-metal in the Anode (diameter 10 mm) and Carbon-coated Al-foil (14 mm) in the positive side was used).

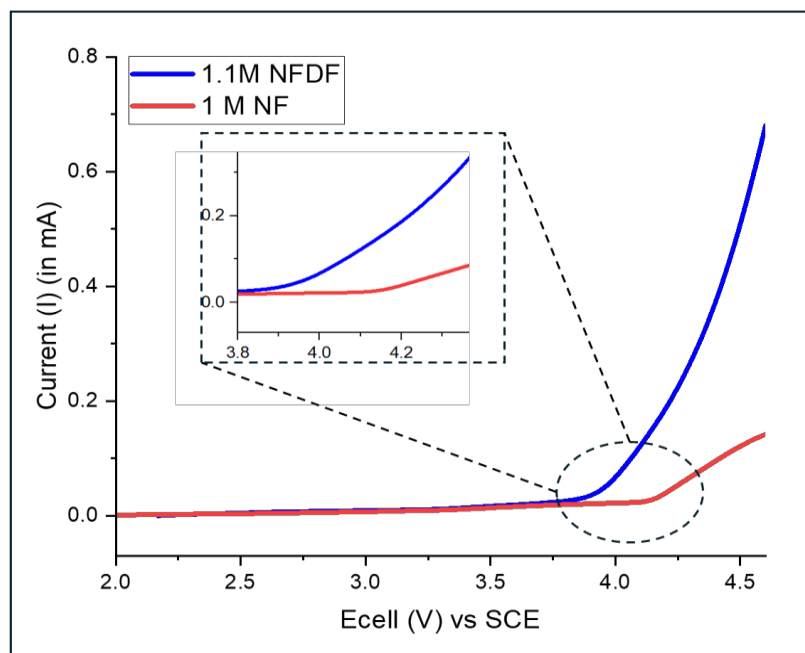


Fig 16. LSV plots for 1M NF (Red line) and 1.1M NFDF (Blue line).

For Cell performance, GCD technique was used to record Capacity by varying Voltage between the two electrodes and keeping a constant current flow. In total four cells of Na-metal as Anode material and NVP as Cathode material as combination (**Na||NVP cells**) for each Electrolyte was assembled. Two of them were subjected to charging and discharging at 0.1C to check their long-term thermodynamic stability..The other two were subjected to rate performance tests to test their kinetic limitations.

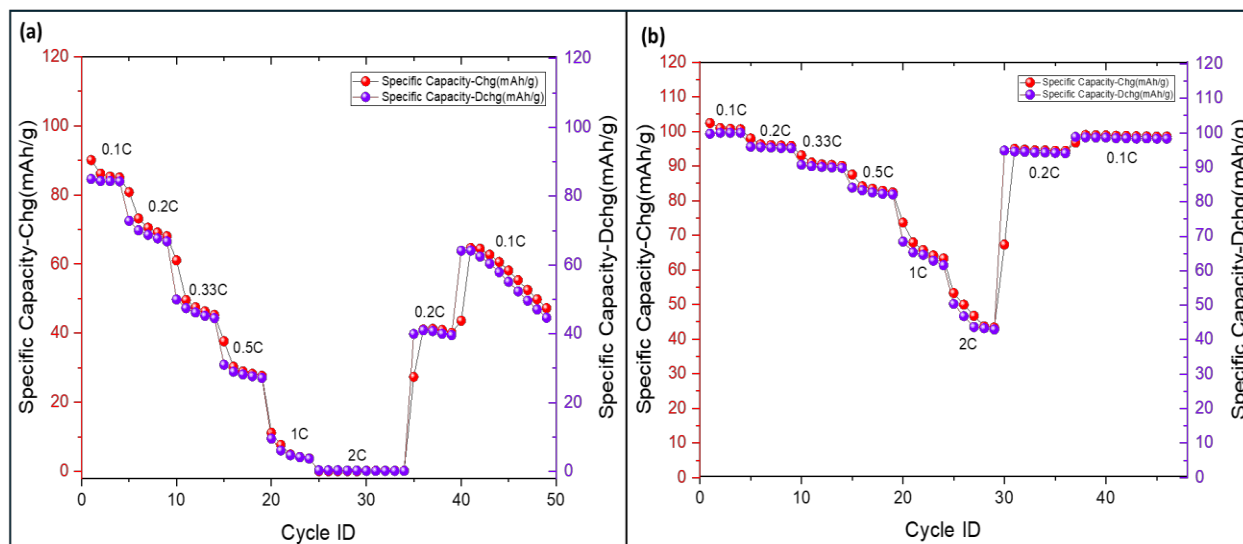


Fig 17. Rate Performance plot for (a) 1M NF and (b) 1.1M NFDF

The cells were cycled between 3.8 V to 2 V inside a constant temperature oven at 298 K.

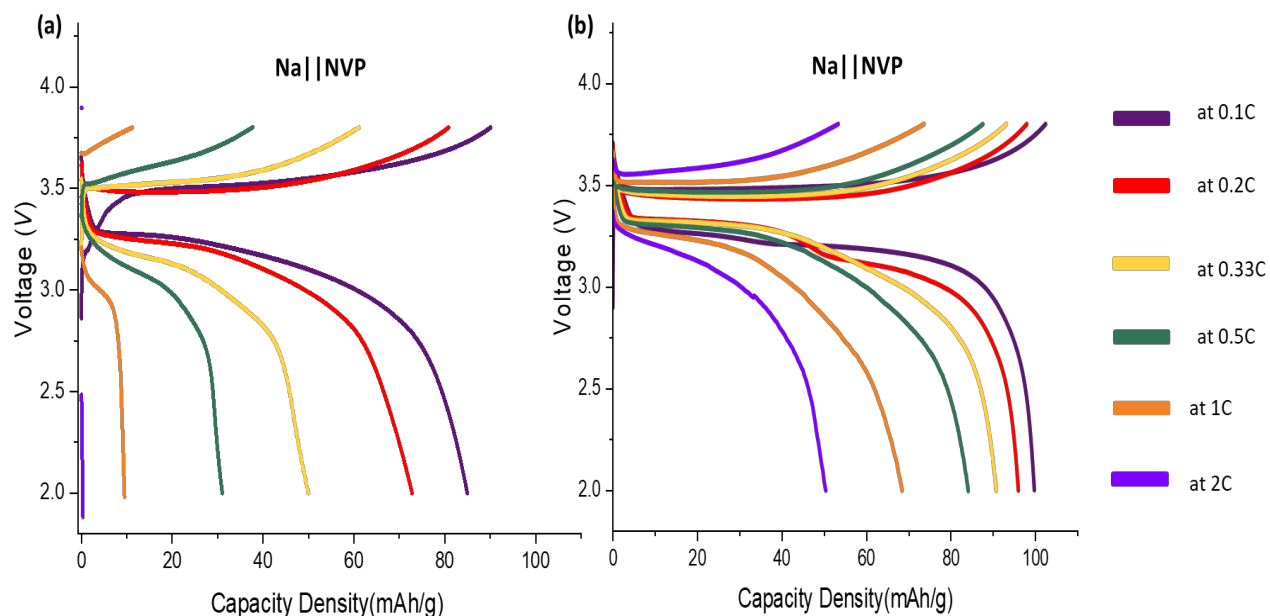


Fig 18. A plot of Charge/Discharge Capacity Density for (a) 1 M NF and (b) 1.1 M NFDF.

Clearly 1 M NF shows a poor rate performance compared to 1.1M NFDF. EIS was conducted after completion of every C-rates. The cells were given significant time at rest before every impedance analysis to ensure mobile ions are at a steady state.

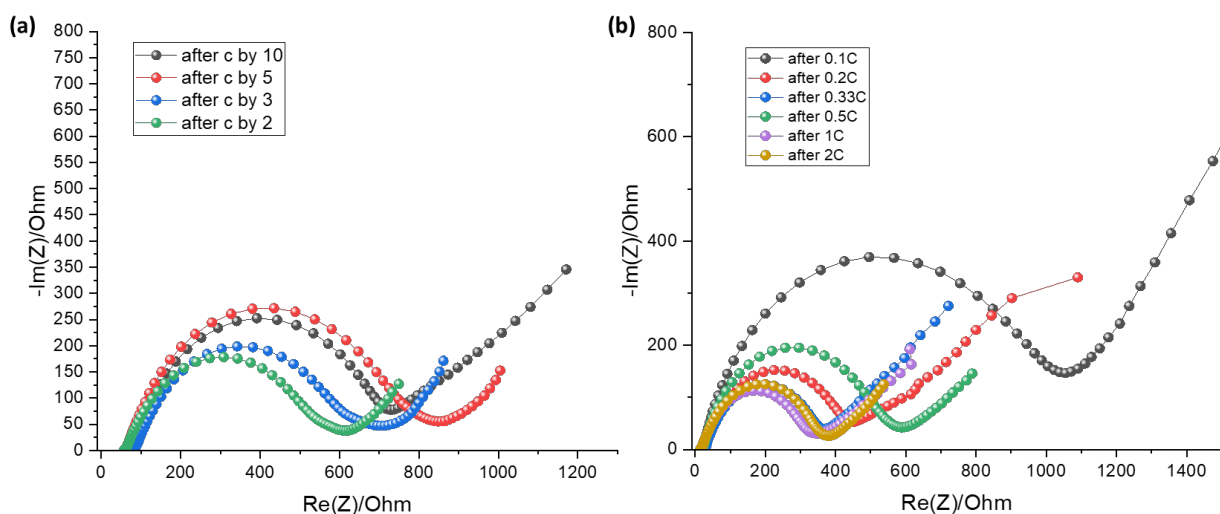


Fig 19. Nyquist plots of impedance analysis after every C-rate of (a) 1M NF and (b) 1.1M NFDF.

Also, some cells were made to obtain their thermodynamic Stability at a very slow C-rate, i.e. 0.1C.

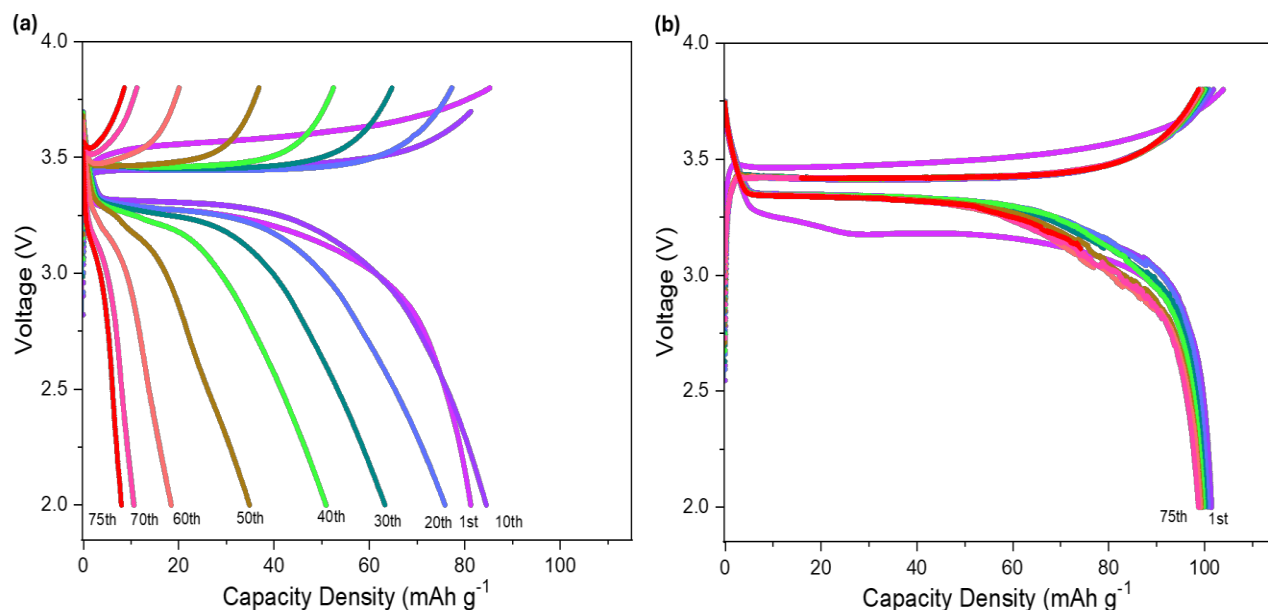


Fig 20. GCD plot of (a) 1 M NF and (b) 1.1M NFDF at 0.1 C for long cycling stability

The 1.1M is still running and Final data will be updated soon

The Raman Spectroscopy analysis of the above two electrolytes were also performed to determine the variation in their ionic species, i.e. Solvation structures. At first, Raman spectra were recorded for the solvents only without any salt or additive to serve as a reference. Then, the spectra for the electrolyte was recorded of a particular range corresponding to the signature peaks of the particular characteristic bonds of the solvents/salts. Since the designed electrolyte had both phosphates and ethers, and their characteristic bond stretching frequency occurs at different regions, both regions were recorded individually for better signal-to-noise ratio.

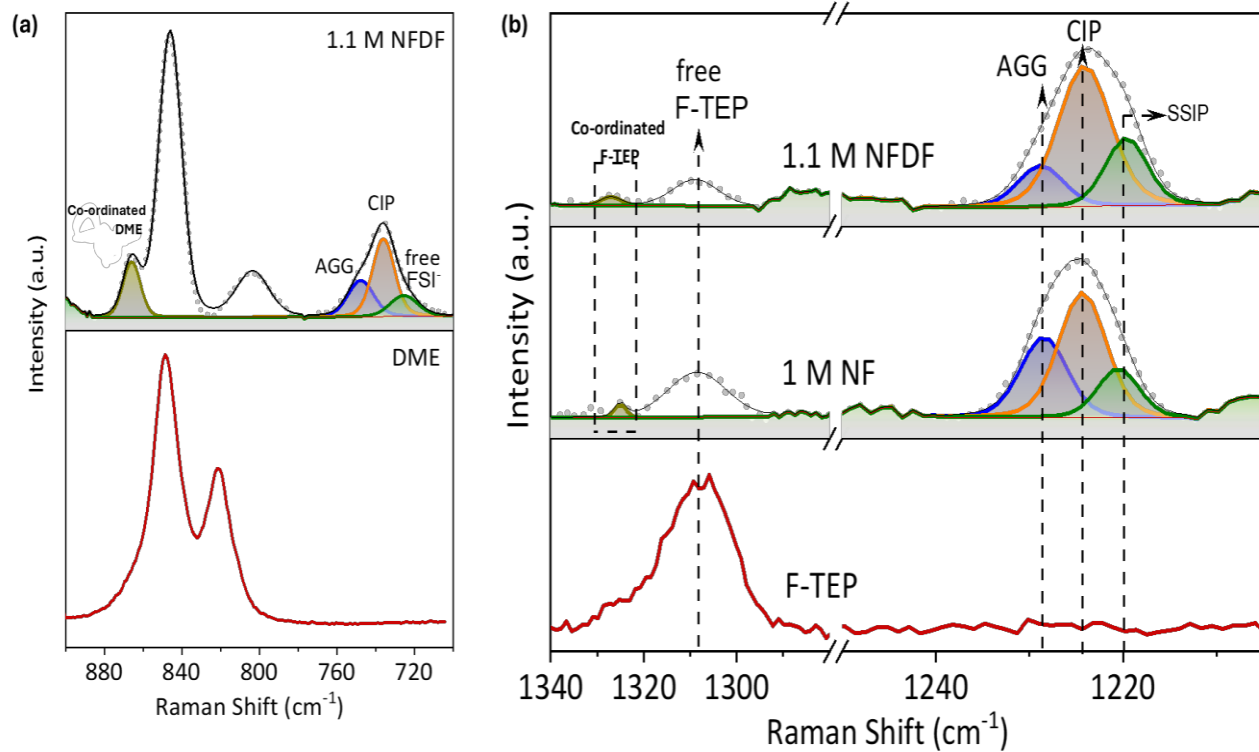


Fig 21. Raman spectra of (a) DME ether region along with the 1.1 M NFDF and (b) FTEP align with 1 M NF and 1.1 M NFDF.

Chapter 4 Discussion

The NaPF_6 salt synthesized had a better yield than the reported paper with modulation of the experimental setup. Characterization was done by solution-state NMR. The ^{31}P NMR and ^{19}F NMR spectra revealed the expected septet and doublet signals at -144.6 ppm and -73.2 ppm respectively. This confirmed the presence of the PF_6^- anion.

However, the ^1H NMR showed some insightful results. Firstly, residual THF peaks were observed at 3.6 ppm and 1.8 ppm respectively. Secondly, it confirmed the absence of any NH_4^+ cation which appears at 5.9 ppm. But, it had an extra intense peak at 2.4 ppm. When the ^1H NMR of NH_4PF_6 salt as purchased from Sigma-Aldrichh was done, the same peak appeared in less intensity. The extra peak was confirmed to be present due to the impurity in the starting material. So, the salt was further dried under an active vacuum for 12 hours. But the peak still persists.

In order to determine the presence of the extra peak at 2.4ppm in the electrolyte, 1 M NaPF_6 in DG was prepared and ^1H Coaxial NMR was performed with D_2O as reference. The salt can be used for making electrolytes If the peak at 2.4ppm is not obtained in the final form as an electrolyte.

- ^1H NMR of 1 M NaPF_6 in DG with D_2O as reference.

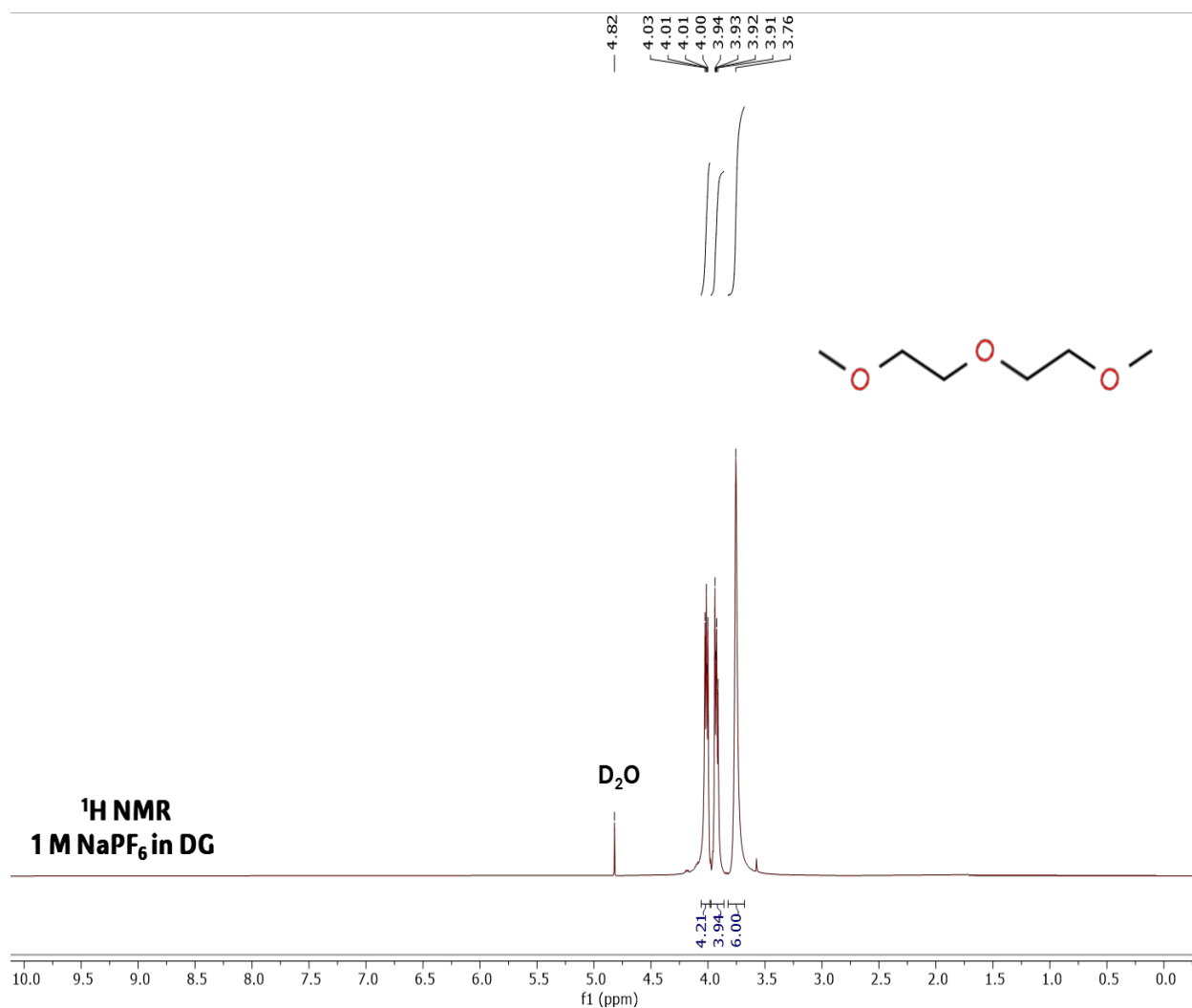


Fig 22. ^1H Coaxial NMR(400 MHz), 1 M NaPF_6 in DG with D_2O as reference.

Clearly, the peak at 2.4ppm is absent in the electrolyte. The peaks at 3.76, 3.9 and 4 ppm correspond to DG. The D_2O peak appears at 4.8 ppm.

Thus, it is safe to conclude that the synthesized NaPF_6 can be readily used to make electrolytes since it has a very-low self-life period.

The screening of electrolytes provided a fundamental understanding of the solubility of various salts of sodium. The ion-dissociation energy of various anions were experimentally determined. The order of decreasing Ion-Dissociation Energy is as follows :-



[W. A. Henderson, J. Phys. Chem. B, 2006, 110, 13177–13183]

This trend conveys that a particular concentration (say 1M) of NaBF₄ is more difficult to solvate than the same concentration of NaPF₆ by a particular organic solvent. Also, the decreasing HOMO level of the Na-salts follows the order of :-



This trend signifies that NaPF₆ has the highest oxidation stability among all the salts. NaPF₆ evolves as a best candidate from the list of salts described above. But the purity and self-life of the salt is a setback for reliable research. If given a careful look at the trend. The next best performing salt is NaFSI. Because of its excellent solubility and good oxidation stability and excellent purity, very high concentration can be reached even in Low-solvating solvents in order for formation of CIPs and AGGs. So, NaFSI was chosen to be the salt under study.

The solvent to be selected for this thesis should be firstly low-solvating, but more importantly Non-flammable as a whole. TEP is a well-known organic solvent marked in literature as a Flame-retardant solvent in electrolytes [a paper from Younes, 16 Xu et al].

The mechanism behind phosphates being non-flammable is that common organic solvents upon heating produce Hydrogen radicals. These hydrogen radicals can further react with the oxygen atom present in solvent molecules to produce Oxygen radicals. This triggers the formation of more free radicals giving rise to a self-sustaining fire by presence of oxygen being evolved inside the cell resulting in combustion. To terminate the self-sustaining reaction, a hydrogen or Oxygen radical scavenger needs to be incorporated. Phosphates are the radical scavengers. The fluorine and phosphorus radical in general

part of the electrolyte decomposition, reacts with Hydrogen radicals and inhibits the radical linear chain reaction.⁴³ [43].

However, TEP is strongly solvation solvent since it can dissolve high amounts (>4 M) of NaFSI salt. Substituting H-atoms in solvent molecules with F-atoms is an excellent strategy to make a solvent Low-solvating in nature. This is due to the mechanism of electronegativity, where F-atoms upon addition, being more electronegative than O-atom, attracts the lone pair of electrons of O-atoms towards itself thereby reducing the polarity of the solvent molecule as a whole. This lowering of polarity of the solvent molecule makes it difficult to dissolve polar inorganic salts. Also, F-atom-containing molecules tend to have a lower HOMO which means a higher oxidation stability and can be applied to higher voltage cathode materials for more capacity density. Fluorination also increases the flash point, boiling point of the molecule in general. So, Fluorinated-TEP was used as the solvent for study.

But, Fluorinated-TEP also has a higher viscosity which can affect Ionic Conductivity and bulk diffusion phenomena. F-TEP can only dissolve $\leq 1.5\text{M}$ of NaFSI. Also the 1.5M NaFSI in FTEP was hazy and highly viscous to be processed as a liquid electrolyte. So instead of a diluent, a Solvating solvent particularly an ether (DME) was added in small quantities until a clear and less viscous electrolyte was formed. DME was chosen because of its excellent solvating ability, compatibility with electrodes and having low density. 5% FEC was added as a film-forming additive. FEC has a very low-lying LUMO compared to other components of this electrolyte system. SO during charging of the cell, FEC is decomposed preferentially on the interface of Anode and the electrolyte forming a film and thereby reducing any further electrolyte decomposition. The final electrolyte formed was 1.1M NaFSI in FTEP: DME (3:1) + 5 vol% FEC (**1.1M NFDF**).

LSV plots show that the developed electrolyte 1.1M NFDF (blue line) has a slightly lower oxidation stability than the Base electrolyte in red line (1M NF). This is due to the fact that the presence of DME decreases oxidation stability of the electrolyte. As DME has a lower

HOMO than FTEP and which results in a lower peak current onset voltage at ~3.87 V in comparison to 4.15 V of 1M NF which contains only FTEP thereby showing higher oxidation stability. LSV gives an experimental stability of Oxidation voltage of the electrolyte and thus helps in determining the combination of electrodes to be used for their testing. Considering the Oxidation Voltage of 1.1M NFDF and 1M NF, $\text{Na}_3\text{V}_2(\text{PO})_4$ (NVP), a NASICON type polyanionic compound as a cathode material can be used. NVP does not give any significant capacity contribution above 3.8 V. The NVP electrochemical activity relies on the redox couple $\text{V}^{4+}/\text{V}^{3+}$, occurring at 3.4 V vs Na^+/Na . In order to increase the conductivity, NVP was carbon-coated as previously done in [54 Thesis]. The loading of the electrode was **5 mg cm⁻²** relative to the existing literature works on Phosphate-based electrolyte (**1 mg cm⁻²**)⁴⁴.

The Na||NVP cells were subjected to GCD studies and their long-cycling stability at low C-rate, i.e 0.1C was tested. The long-cycling at low C-rate is carried out to test the thermodynamic stability of the electrolyte because the system is given ample time to ensure kinetic limitations do not occur and to allow chemical reaction if it exists. If there exists a significant capacity fading with an increasing cycle number. It can be validated that the electrolyte undergoes chemical reactions other than redox phenomena resulting in loss of Na-inventory. Fig. 20 clearly shows the poor stability of the 1M NF electrolyte since it has a drastic capacity fading after 55 cycles with a **capacity fade of 90%** after just 75 cycles. Whereas the designed electrolyte performs exceptionally at 0.1C with **capacity fade** of only **3%** after 75 cycles. The **1.1M NFDF Na||NVP** cell is still running, and the data will be updated in due course. In addition, the hysteresis corresponding the difference between the oxidation and reduction plateau of Vanadium in cathode material during the charge discharge cycle curves decreases with further cycling in the 1.1M NFDF electrolyte containing cells.

The rate performance was also tested by sequentially increasing the C-rate. Even in the rate performance GCD analysis, 1.1 M NFDF performed better in comparison to 1 M NF. The 1.1 M NFDF cell had a **capacity retention of 65%** in comparison to 1 M NF cell with a **capacity retention** of only **11%** after 1C. In fact, 1 M NF dies off at 2C current rate whereas the 1.1M NFDF continues to give better performance as depicted in Fig 17. and Fig 18.

The 1.1M NFDF also delivered a better first cycle Capacity Density of 102.8 mAh g⁻¹ compared to 85.6 mAh g⁻¹ of 1 M NF cells. It is worth noting that the I.C.E of 1.1 M NFDF cells is 97.4% in contrast to the lower I.C.E of 1 M NF cells at 94.3%.

Fig 19. Shows the Nyquist plot of Impedance analysis carried out on both the electrolytes. The starting point of the semicircle on the x-axis refers to the solution resistance (R_s) of the electrolyte. So, the closer it is to zero on the x-axis, the lower is the resistance provided by the electrolyte along with greater ionic conductivity. As the result shows, the 1.1M NFDF has R_s near to zero compared to R_s of 1 M NF clearly indicating better ionic conductivity and lower resistance contribution. The following semicircle post- R_s is a summation of all charge-transfer limiting processes at the interface. Smaller the semicircle, the better the charge-transfer kinetics.

With increasing C-rate, 1.1 M NFDF shows a reduction in the semicircle indicating that the charge-transfer processes at the interface are more facile. The decrease in R_{CT} also reflects the formation of a stable SEI after 0.1C. 1 M NF produces similar and a larger magnitude R_{CT} compared to 1.1M NFDF. The 45° inclined line after the semicircle is assigned to Bulk-diffusion processes occurring at longer timescales or lower frequency regions.

Raman Analysis was performed inside a inert Ar-filled Glove Box with H₂O and O₂ content less than 0.1 ppm in order to understand the nature of the ionic species being formed which results in the exceptional stability of the electrolyte. In Fig 21., as the electrolyte 1.1 M NFDF had a mixture of both Phosphates and Ethers, the characteristics P=O stretching vibration band of free FTEP occurs at 1308 cm⁻¹ as evident from the bare FTEP Raman spectra. New peak arises when salt is added at a higher wavenumber due to the coordination of FTEP with Na⁺. The peak that are recorded at the range in the range 1220-1230 cm⁻¹ are the region assigned to the S=O stretching vibration which belong to the FSI⁻ anion. Deconvoluting the peaks gives the composition of CIPs, SSIPs and AGGs formed due to the low-solvating FTEP. In the Ether zone, only peaks from 1.1 M NFDF is recorded since 1 M NF does not have any ether as solvent. The peaks at 784 cm⁻¹, is assigned to the C-O-C stretching vibration of the DME molecule. The peaks at the region from 720-750 cm⁻¹ reveal the contribution of DME in forming CIPs, SSIPs and AGGs.

Both FTEP and DME contribute to the formation of ionic species by participating in the solvation process. Both regions show the presence of more amount of CIPs which will contribute to the formation of Anion-derived inorganic-rich SEI thereby, proving the exceptional stability of 1.1 M NFDF.

In Conclusion, all the Electrochemical and analytical results show the exceptional performance of the designed electrolyte.

Lastly, Non-Flammability test was carried out of GF-F separators dipped in an electrolyte of 1 M NaPF_6 in EC:DEC (1:1), a conventional electrolyte and in 1.1 M NFDF. Fig 23. shows the results of the non-flammability tests.

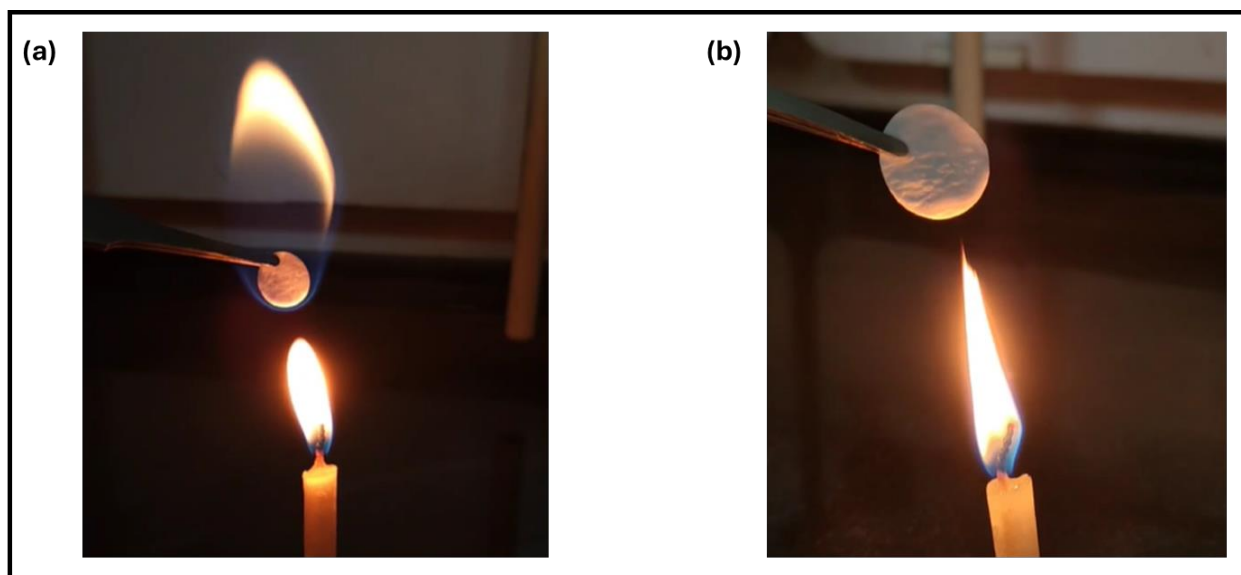


Fig 23. Non-flammability tests of (a) 1 M NaPF_6 in EC:DEC (1:1) and (b) 1.1M NFDF.

Reference

1. Whittingham, M.S. (2012). History, evolution, and future status of energy storage. In Proceedings of the IEEE (Institute of Electrical and Electronics Engineers Inc.), pp. 1518–1534. 10.1109/JPROC.2012.2190170.
2. Tarascon, J.M. (2010). Is lithium the new gold? Preprint, 10.1038/nchem.680 10.1038/nchem.680.
3. Vikström, H., Davidsson, S., and Höök, M. (2013). Lithium availability and future production outlooks. *Appl Energy* 110, 252–266. 10.1016/j.apenergy.2013.04.005.
4. Armand, M., and Tarascon, J.-M. (2008). Building better batteries. *Nature* 451, 652–657. 10.1038/451652a.
5. Ponrouch, A., Monti, D., Boschini, A., Steen, B., Johansson, P., and Palacín, M.R. (2015). Non-aqueous electrolytes for sodium-ion batteries. *J Mater Chem A Mater* 3, 22–42. 10.1039/C4TA04428B.
6. Palomares, V., Serras, P., Villaluenga, I., Hueso, K.B., Carretero-González, J., and Rojo, T. (2012). Na-ion batteries, recent advances and present challenges to become low cost energy storage systems. Preprint, 10.1039/c2ee02781j 10.1039/c2ee02781j.
7. Mahmoudzadeh Andwari, A., Pesiridis, A., Rajoo, S., Martinez-Botas, R., and Esfahanian, V. (2017). A review of Battery Electric Vehicle technology and readiness levels. Preprint at Elsevier Ltd, 10.1016/j.rser.2017.03.138 10.1016/j.rser.2017.03.138.
8. Scrosati, B. (2011). History of lithium batteries. Preprint, 10.1007/s10008-011-1386-8 10.1007/s10008-011-1386-8.
9. Zschornak, M., Meutznier, F., Lück, J., Latz, A., Leisegang, T., Hanzig, J., Nentwich, M., Zosel, J., and Balbuena, P.B. (2019). Fundamental principles of battery design. Preprint at De Gruyter, 10.1515/psr-2017-0111 10.1515/psr-2017-0111.
10. Zhang, L., Li, X., Yang, M., and Chen, W. (2021). High-safety separators for lithium-ion batteries and sodium-ion batteries: advances and perspective. Preprint at Elsevier B.V., 10.1016/j.ensm.2021.06.033 10.1016/j.ensm.2021.06.033.
11. Larcher, D., and Tarascon, J.M. (2015). Towards greener and more sustainable batteries for electrical energy storage. Preprint at Nature Publishing Group, 10.1038/nchem.2085 10.1038/nchem.2085.
12. Tarascon, J.M. (2020). Na-ion versus Li-ion Batteries: Complementarity Rather than Competitiveness. Preprint at Cell Press, 10.1016/j.joule.2020.06.003 10.1016/j.joule.2020.06.003.
13. Bauer, A., Song, J., Vail, S., Pan, W., Barker, J., and Lu, Y. (2018). The Scale-up and Commercialization of Nonaqueous Na-Ion Battery Technologies. *Adv Energy Mater* 8. 10.1002/aenm.201702869.
14. Hijazi, H., Desai, P., and Mariyappan, S. (2021). Non-Aqueous Electrolytes for Sodium-Ion Batteries: Challenges and Prospects Towards Commercialization. Preprint at John Wiley and Sons Inc, 10.1002/batt.202000277 10.1002/batt.202000277.
15. Chombo, P.V., and Laoonual, Y. (2020). A review of safety strategies of a Li-ion battery. *J Power Sources* 478, 228649. <https://doi.org/10.1016/j.jpowsour.2020.228649>.

16. Hu, Y.S., and Lu, Y. (2020). The Mystery of Electrolyte Concentration: From Superhigh to Ultralow. Preprint at American Chemical Society, 10.1021/acsenergylett.0c02234 10.1021/acsenergylett.0c02234.
17. Ma, Q., and Tietz, F. (2020). Solid-State Electrolyte Materials for Sodium Batteries: Towards Practical Applications. Preprint at Wiley-VCH Verlag, 10.1002/celc.202000164 10.1002/celc.202000164.
18. Gebert, F., Knott, J., Gorkin, R., Chou, S.L., and Dou, S.X. (2021). Polymer electrolytes for sodium-ion batteries. *Energy Storage Mater* 36, 10–30. 10.1016/j.ensm.2020.11.030.
19. Li, Y., Wu, F., Li, Y., Liu, M., Feng, X., Bai, Y., and Wu, C. (2022). Ether-based electrolytes for sodium ion batteries. Preprint at Royal Society of Chemistry, 10.1039/d1cs00948f 10.1039/d1cs00948f.
20. Read, J., Mutolo, K., Ervin, M., Behl, W., Wolfenstine, J., Driedger, A., and Foster, D. (2003). Oxygen Transport Properties of Organic Electrolytes and Performance of Lithium/Oxygen Battery. *J Electrochem Soc* 150, A1351. 10.1149/1.1606454.
21. Wang, E., Niu, Y., Yin, Y.X., and Guo, Y.G. (2021). Manipulating Electrode/Electrolyte Interphases of Sodium-Ion Batteries: Strategies and Perspectives. Preprint at American Chemical Society, 10.1021/acsmaterialslett.0c00356 10.1021/acsmaterialslett.0c00356.
22. Goodenough, J.B. (2014). Electrochemical energy storage in a sustainable modern society. Preprint at Royal Society of Chemistry, 10.1039/c3ee42613k 10.1039/c3ee42613k.
23. Peljo, P., and Girault, H.H. (2018). Electrochemical potential window of battery electrolytes: The HOMO-LUMO misconception. *Energy Environ Sci* 11, 2306–2309. 10.1039/c8ee01286e.
24. Wang, A., Kadam, S., Li, H., Shi, S., and Qi, Y. (2018). Review on modeling of the anode solid electrolyte interphase (SEI) for lithium-ion batteries. Preprint at Nature Publishing Group, 10.1038/s41524-018-0064-0 10.1038/s41524-018-0064-0.
25. Paled, E. The Electrochemical Behavior of Alkali and Alkaline Earth Metals in Nonaqueous Battery Systems-The Solid Electrolyte Interphase Model.
26. Gond, R., Van Ekeren, W., Mogensen, R., Naylor, A.J., and Younesi, R. (2021). Non-flammable liquid electrolytes for safe batteries. *Mater Horiz* 8, 2913–2928. 10.1039/d1mh00748c.
27. Li, Z., Rao, H., Atwi, R., Sivakumar, B.M., Gwalani, B., Gray, S., Han, K.S., Everett, T.A., Ajantiwalay, T.A., Murugesan, V., et al. (2023). Non-polar ether-based electrolyte solutions for stable high-voltage non-aqueous lithium metal batteries. *Nat Commun* 14. 10.1038/s41467-023-36647-1.
28. Speight, J.G. (2020). 3 - Water chemistry. In *Natural Water Remediation*, J. G. Speight, ed. (Butterworth-Heinemann), pp. 91–129. <https://doi.org/10.1016/B978-0-12-803810-9.00003-6>.
29. Von Cresce, A., and Xu, K. (2011). Preferential solvation of Li⁺ directs formation of interphase on graphitic anode. *Electrochemical and Solid-State Letters* 14. 10.1149/1.3615828.
30. Zhang, X.Q., Chen, X., Hou, L.P., Li, B.Q., Cheng, X.B., Huang, J.Q., and Zhang, Q. (2019). Regulating Anions in the Solvation Sheath of Lithium Ions for Stable Lithium Metal Batteries. *ACS Energy Lett* 4, 411–416. 10.1021/acsenergylett.8b02376.

31. Hu, Y.S., and Pan, H. (2022). Solvation Structures in Electrolyte and the Interfacial Chemistry for Na-Ion Batteries. Preprint at American Chemical Society, 10.1021/acsenergylett.2c02529 10.1021/acsenergylett.2c02529.
32. Tian, Z., Zou, Y., Liu, G., Wang, Y., Yin, J., Ming, J., and Alshareef, H.N. (2022). Electrolyte Solvation Structure Design for Sodium Ion Batteries. Preprint at John Wiley and Sons Inc, 10.1002/advs.202201207 10.1002/advs.202201207.
33. Saito, T., Nakaie, S., Kinoshita, M., Ihara, T., Kinugasa, S., Nomura, A., and Maeda, T. (2004). Practical guide for accurate quantitative solution state NMR analysis. *Metrologia* 41, 213–218. 10.1088/0026-1394/41/3/015.
34. Cheng, F., Cao, M., Li, Q., Fang, C., Han, J., and Huang, Y. (2023). Electrolyte Salts for Sodium-Ion Batteries: NaPF₆ or NaClO₄? *ACS Nano* 17, 18608–18615. 10.1021/acsnano.3c07474.
35. Barnes, P., Smith, K., Dufek, E.J., Jones, C., Skinner, P., Storch, E., White, Q., Deng, C., Karsann, D., Lau, M.L., et al. (2020). A non-aqueous NaPF₆-based electrolyte degradation study: formation and mitigation of HF.
36. Terborg, L., Nowak, S., Passerini, S., Winter, M., Karst, U., Haddad, P.R., and Nesterenko, P.N. (2012). Ion chromatographic determination of hydrolysis products of hexafluorophosphate salts in aqueous solution. *Anal Chim Acta* 714, 121–126. 10.1016/j.aca.2011.11.056.
37. Bhide, A., Hofmann, J., Katharina Dürr, A., Janek, J., and Adelhelm, P. (2014). Electrochemical stability of non-aqueous electrolytes for sodium-ion batteries and their compatibility with Na_{0.7}CoO₂. *Physical Chemistry Chemical Physics* 16, 1987–1998. 10.1039/c3cp53077a.
38. Ould, D.M.C., Menkin, S., O’Keefe, C.A., Coowar, F., Barker, J., Grey, C.P., and Wright, D.S. (2021). New Route to Battery Grade NaPF₆ for Na-Ion Batteries: Expanding the Accessible Concentration. *Angewandte Chemie - International Edition* 60, 24882–24887. 10.1002/anie.202111215.
39. Murray, V., Hall, D.S., and Dahn, J.R. (2019). A Guide to Full Coin Cell Making for Academic Researchers. *J Electrochem Soc* 166, A329–A333. 10.1149/2.1171902jes.
40. Kim, T., Choi, W., Shin, H.C., Choi, J.Y., Kim, J.M., Park, M.S., and Yoon, W.S. (2020). Applications of voltammetry in lithium ion battery research. Preprint at Korean Electrochemical Society, 10.33961/jecst.2019.00619 10.33961/jecst.2019.00619.
41. Lazanas, A.C., and Prodromidis, M.I. (2023). Electrochemical Impedance Spectroscopy—A Tutorial. Preprint at American Chemical Society, 10.1021/acsmeasuresciau.2c00070 10.1021/acsmeasuresciau.2c00070.
42. Pinder, J.W., Major, G.H., Baer, D.R., Terry, J., Whitten, J.E., Čechal, J., Crossman, J.D., Lizarbe, A.J., Jafari, S., Easton, C.D., et al. (2024). Avoiding common errors in X-ray photoelectron spectroscopy data collection and analysis, and properly reporting instrument parameters. *Applied Surface Science Advances* 19. 10.1016/j.apsadv.2023.100534.
43. Nagasubramanian, G., and Fenton, K. (2013). Reducing Li-ion safety hazards through use of non-flammable solvents and recent work at Sandia National Laboratories. Preprint, 10.1016/j.electacta.2012.09.065 10.1016/j.electacta.2012.09.065.
44. Li, H., Chen, H., Shen, X., Liu, X., Fang, Y., Zhong, F., Ai, X., Yang, H., and Cao, Y. (2022). High-Voltage and Intrinsically Safe Sodium Metal Batteries Enabled by

Nonflammable Fluorinated Phosphate Electrolytes. ACS Appl Mater Interfaces 14, 43387–43396. 10.1021/acsami.2c13295.